

## Experimental Evaluation of the T100-3 Stationary Plasma Thruster and Xenon Propellant System For The RHETT- 1 Program

Charles E. Garner\* and Juergen Mueller\*  
 Jet Propulsion Laboratory  
 California Institute of Technology  
 Pasadena, Ca 91109

Anatoly Vasin\*, Mikhail Lasinsky\*, and Valery Petrosov\*  
 Keldysh Research Institute for Thermal Processes  
 Moscow, Russia

### ABSTRACT

AT-100-3 Russian Hall plasma thruster, xenon flow control unit (XFCU) and US xenon propellant subsystem developed for the RHETT-1 propulsion system are described. The propellant system includes a pressure regulator, on/off valves, service valve and high/low pressure transducers, built to flight-like standards and assembled onto a mounting plate structure. Testing of the propellant system included experiments to measure output pressure regulation variations through a temperature range of -20 through +30 degrees C with an input pressure range of 413-6100 kPa (60-885 PSI A). A Russian-designed and fabricated laboratory xenon flow control unit was evaluated over a range of XFCU temperatures, input pressures, and flow rates. The thruster evaluation program included performance testing at various discharge voltage and input power levels, and a 632-hour wear test. Thrust and efficiency of the T-100-3 are comparable to the SPT-100. The endurance test was performed for 349 on/off cycles and 632.4 hours of operation at an input power to the thruster of approximately 1.35 kW. Each cycle was nominally 24 hours of thruster on-time and 10 minutes of thruster off-time. Thrust and thruster efficiency decreased, from 83 mN and 49% at BOL to 81.5 mN and 45% at the completion of the wear test. Thruster mass decreased by approximately 20 g over 630 hours. Over the course of the wear test the peak beam current density in the thruster plume measured on the thruster centerline decreased only slightly. T-100-3 plume characteristics are similar to those measured on the SPT-100. Inner insulator wear rates were a factor of three lower and outer insulator wear rates at certain locations were 30% greater than the insulator wear rates measured on the SPT-100. Life estimates for the T-100-3 based on the wear test data are consistent with life estimates of the SPT-100. The flight-like propellant feed system, T-100-3 thruster, and laboratory xenon flow control unit were tested together as a system in vacuum; all subsystems functioned nominally. The thruster, XFCU and XPS then were subsequently integrated into the RHETT-1 propulsion system at Lewis Research Center and tested with a power processing unit and integrated structure.

### INTRODUCTION

Stationary plasma thrusters are gridless ion thrusters that were originally investigated in the US in the early 1960's [1-3]. However, it was in the former Soviet Union that these thrusters were developed to operate efficiently and were ultimately optimized to operate at a specific impulse of approximately 1,600 s with an efficiency of over 0.5 [4-6]. The SPT was successfully developed during the 1960's and 1970's by Morozov and others to obtain a unique combination of specific impulse and efficiency. Sixty-four SPT-60 and SPT-70 thrusters have flown in space, starting with the Meteor 1 in 1969-1970 [7-9]. The mission success rate for these thrusters is reported to be 100% [9]. More recently, 8 SPT-100 thrusters each were flown on the Russian GALS and EXPRESS satellites [9]. Reportedly all thruster systems are functioning nominally [10].

\* Member of the Technical Staff, Advanced Propulsion Technology Group.

+ Keldysh Research Institute of Thermal Processes

In 1990 the former USSR began to make available to the West data concerning the unique characteristics of these Hall thrusters. In 1991, under a program sponsored by the Ballistic Missile Defense Organization (BMDO) a team of electric propulsion specialists visited the USSR to experimentally evaluate the performance of a 1.35-kW SPT at the Scientific Research Institute of Thermal Processes in Moscow and at Design Bureau "Fakel" in Kaliningrad, Russia. The evaluation verified that the actual performance of the thruster was close to the claimed performance of 50% efficiency at a specific impulse of 1600 s [11]. Studies indicate that for north/south station keeping and Earth orbit raising applications of electric propulsion, the optimum specific impulse is in the range of 1,000-2,000 sec [12]. The combination of the flight heritage of the SPT-70 and the availability of thrusters and thruster data led to substantial interest in these thrusters by Western spacecraft manufacturers for primary and auxiliary propulsion applications. Space Systems/Loral is presently flight-qualifying SPT-100 thrusters for north/south station keeping and Earth orbit raising applications and plans to provide these thrusters on their

spacecraft [13]. Recently Design Bureau Fakel, located in Kaliningrad, Russia, successfully completed a 7,000-hr endurance test of an SPT-100 [14].

Since the initial visit to the former Soviet Union in 1991 BMDO has pioneered the introduction of this technology to the west through a variety of programs and activities that include support of Space Systems/Loral's SPT-100 qualification program [15-18], evaluation of the thruster with anode layer [19-21], testing of high-power Hall thrusters [22-24], and development of a prototype Hall thruster electric propulsion system called RHETT-1 (Russian Hall Effect Thruster Technology) [25,26]. BMDO's objective is to develop new electric propulsion technology and support commercialization of that technology through development programs and flight projects.

As part of the BMDO-sponsored test program the T-100-3 thruster from the Keldysh Research Institute for Thermal Processes (NIITP) was evaluated. NIITP began work in electric propulsion in 1960 [27]; early efforts centered on multi-mega watt MPD propulsion. By the 1970's thruster development had outpaced power availability in space and NIITP's program was re-directed towards development of laboratory and flight plasma sources for space physics investigations, ground applications for ion sources, and ion sources for controlled thermonuclear fusion. Plasma sources developed at NIITP flew as payloads on various missions including Cosmos-728, Cosmos 780, and numerous sounding rocket flights. Ultimately NIITP focused on the development of advanced Hall electric thrusters with a variety of testing and analysis activities that are described in Ref. 27. Chief among these activities at NIITP are the development of heaterless hollow cathodes [27], an advanced SPT-100 plasma thruster called the T-100-3 [27], and an advanced propellant flow control system. NIITP has completed wear tests [28] and electromagnetic interference measurements [29] of the T-100-3 thruster, and 20,000 on/off cycles and a 1,500-hr wear test of the heaterless hollow cathode [28].

In 1995 BMDO tasked the Lewis Research Center (LeRC) to develop RHETT-1 (Russian Hall Effect Thruster Technology), an integrated Hall electric thruster propulsion system [26]. The goal of this program was to build a system as flight-like as possible that would reduce the cost and risk of developing flight Hall thruster systems. The T-100-3 from NIITP was selected for this system.

JPL's responsibilities in the RHETT-1 program were to procure and test the propellant storage and distribution system (PSDS), evaluate a xenon flow control unit (XFCU) designed and fabricated at NIITP, evaluate and wear test the T-100-3 plasma thruster, test these three subsystems together as an integrated system, and provide these subsystems to LeRC to be integrated into the RHETT-1 propulsion system. The thruster, XFCU and XPS then were subsequently integrated into RHETT-1 at Lewis Research Center and tested with a

power processing unit and integrated structure [26]. This paper presents the results of an evaluation of the PSDS, the XFCU, and the T-100-3. Results of a 630-hr thruster wear test are also described.

## APPARATUS

A photograph of the T-100-3 plasma thruster developed at NIITP and used for the RHETT-1 evaluation is shown in Fig. 1. The T-100-3 included two heaterless hollow cathodes and had been operated at NIITP for approximately 20 hours prior to testing at JPL. The outer insulator which forms the outside discharge chamber wall was approximately 121.9 mm-dia, and the outer diameter of the inner insulator was 69.8 mm. The thickness of the outer and inner insulators were 10.8 mm and 9.0 mm respectively. In the 630-hr endurance test the cathode at the top (cathode #1) was used as the primary cathode. The unused cathode (cathode #2) was covered with a tantalum shroud to reduce contamination to this cathode during the wear test.

The endurance test was performed in a 3.1-m dia. x 5.1-m stainless steel vacuum chamber equipped with three, each, 1.2-m diameter helium cryopumps. The minimum no-load tank pressure  $8.4 \times 10^{-6}$  Pa ( $8.4 \times 10^{-8}$  Torr). The measured pumping speed on xenon for the three pumps combined is approximately 48,000 l/s. A probe rake, consisting of 25 Faraday probes of diameter 2.3 cm, mounted on a semicircular arc 2.4 m in diameter was used to examine the thruster exhaust. The facility and plume probes are described in detail in Ref. 30.

The thruster was mounted near one end of the vacuum tank, directly facing a cryopump positioned at the other end of the chamber. A chevron-shaped beam target was placed at the opposite end of the vacuum chamber to reduce backspattering of beam target material to the thruster and is described more completely in Ref. 30. Due to the beam divergence characteristics of Hall thrusters, material can also be sputtered from the vacuum tank sidewalls and deposited onto the thruster. Therefore the cylindrical side walls of the vacuum chamber were also lined with graphite panels. Glass slides were placed 21 cm to either side of the thruster such that material back sputtered to the thruster could be quantified and characterized. A photograph of the T-100-3 mounted inside the vacuum chamber is shown in Fig. 2.

Tank pressure was measured using two ion gauges. One gauge tube was mounted to the side wall of vacuum tank; the other tube was mounted inside the vacuum tank, approximately 0.51 m above and 0.58 m behind thruster. This tube was calibrated on both xenon and nitrogen using a spinning rotor gauge that is traceable to the National Institute for Standards and Technology (NIST).

A laboratory propellant system was used for supplying xenon to the T-100-3 for the endurance test and is described in Ref. 30. The xenon supply pressure was

measured using a capacitance manometer that was calibrated to an accuracy of  $\pm 0.25\%$  at 249.94 kPa. Micrometer valves located inside the vacuum chamber were used to control the flow rates to the discharge chamber and cathode. The pressure in the propellant tubing was above atmospheric pressure up to the micrometer valves. This design may prevent cathode poisoning because those parts of the propellant system that are below atmospheric pressure are located inside the vacuum chamber. The purity of the xenon used by the T-100-3 was tested directly from the xenon bottle. Sample data indicate that the purity specifications (99.999%) were exceeded. Finally a xenon purifier supplied by NITP was placed immediately upstream of thruster inside the vacuum system.

Thermal mass flow meters were used to measure the discharge, and total propellant flow rates. The cathode flow rate was calculated by subtracting the discharge flow from the total flow rate. The flow meters were calibrated using a bubble volumeter which was tested at NIST. Test data indicated that at the nominal xenon flow rate of the T-100-3 (approximately 55 sccm) the flow rate measured with the JPL bubble volumeter was approximately 1% lower than the flow rate measured with NITP equipment [31]. The difference is attributed to diffusion of xenon through a rubber hose used in the JPL bubble volumeter. The bubble volumeter data on xenon were curve fit and the curve fit was incorporated into the SPT data acquisition and control program. Flow rate calibrations were performed approximately every 100 hours.

The T-100-3 was mounted to an inverted pendulum style thrust stand of the type developed at NASA LeRC [32]. In this design, thrust is indicated by a linear voltage displacement transducer (LVDT). The thrust stand was surrounded by a water-cooled housing to minimize thermal effects on the measured thrust; the thrust stand housing can be seen just below the T-100-3 in Fig. 2. The thruster was mounted to the thrust stand but was electrically isolated from the thrust stand and facility ground. The T-100-3 was radiation-cooled through use of an aluminum plate that was flocced with carbon fibers to increase its emissivity [33]. Thermocouples were attached to the thruster body and to the radiator plate center and radiator plate corner. The thrust stand inclination was adjusted continuously under computer control to improve the accuracy of the thrust measurement over extended test times. Inward-weight thrust stand calibrations were performed in-situ throughout the wear test. Repeatability of thrust stand calibrations was  $\leq 1.5\%$ .

Thrust is determined from the difference in the LVDT voltage with the thruster on and off. The most accurate way to determine the "thruster off" LVDT voltage is to measure the LVDT voltage within one second of the thruster being turned off; in this way thrust stand drift due to thermal or other effects are minimized. However, thrust measured using this procedure does not include the small thrust element due to expansion of hot xenon out of

the thruster. Total thrust measurements for the T-100-3 reported herein are the sum of the electrostatic thrust plus an estimate of the thrust provided by the hot xenon flowing through the thruster. The estimate for thrust due to expansion of hot xenon out of the thruster was calculated using the following formula:

$F = M_d(8kT / \pi m)^{1/2}$ , where

$F$  = Thrust due to expansion of xenon out of the T-100 (N)

$M_d$  = Discharge flow rate (Kg/s)

$k$  = Boltzman's constant

$T$  = T-100 body temperature (K)

$m$  = Xenon mass ( $2.18 \times 10^{-25}$  Kg)

The thruster was operated using laboratory power supplies for the discharge and cathode ignitor. The discharge voltage was fixed at approximately 300 V. An output filter designed and fabricated by Space Power, Inc. was placed across the thruster anode/cathode to reduce the amplitude of discharge current and voltage oscillations. The thruster was turned on when the cathode was ignited. Thruster starting was performed manually. The discharge current was used to supply the excitation current required for the thruster electromagnet coils.

A DC high voltage start supply across the ignitor and cathode emitter was used to start the cathode. The heaterless NITP hollow cathode is started at room temperature without any preconditioning of the cathode emitter. NITP has demonstrated over 20,000 on/off cycles and 1,500 hours of steady-state testing of their heaterless cathode [28]. NITP now offers a version of their hollow cathode that includes a cathode conditioning heater [34]. The cathode was started at a flow rate of approximately 2 mg/s, and after thruster ignition the cathode flow rate was reduced to the nominal operating value of 0.37 mg/s.

Steady-state thruster operation and shutdown sequencing were controlled by a PC based data acquisition (DAC) system. This system also monitored the vacuum facility enabling unattended operation. A total of 56 channels that included thrust, xenon mass flow rate, anode voltage, and current, floating voltage, magnet current, tank pressure and various other facility components were monitored and recorded as a function of time. The data were averaged in real time and the averaged values were displayed on a monitor and recorded on the computer hard disk drive every 3-60 seconds; higher data recording rates were used during the first 30 minutes and last 5 minutes of thruster operation to examine various thruster operating characteristics and to obtain more precise thrust measurements.

If certain engine or facility parameters exceeded specifications, the computer opened a relay between the thruster anode and the discharge power supply to terminate thruster operation, and activated a telephone dialing machine (autodialer). Xenon flow through the cathode and discharge remained on; there was no active computer

control of the flow rates to the anode and cathode. The computer sent a change-of-state signal every 15 seconds to an electronic timer (heartbeat box); in the event of a computer failure, the timer activated a series of relays to remove PCU power and activated the autodialer. The data storage interval during thruster operation was typically every thirty seconds. The data storage rate during thruster start-up and shutdown was increased to every three seconds to improve thrust measurement accuracy and to record transient thruster data.

Discharge current and electromagnet current were measured using calibrated current shunts. The discharge current calibration was determined using a voltmeter which averages the direct-current value of the discharge current shunt voltage drop over a period of four seconds. Oscillations in the discharge current were measured with an inductive probe placed on the discharge current cable close to the vacuum tank feed through. The discharge voltage ripple was measured at the vacuum tank feed throughs as well, using a combination inductive/Hall effect probe. Cabling length between the vacuum chamber feed through and T100-3 was approximately 6 m,

The thruster was photographed (from an off-axis view) periodically through a window in the vacuum system to document the condition of the thruster. Insulator thicknesses were determined from photographs by measuring the ratio of insulator width to the outer diameter of the outer insulator or inner diameter of the inner insulator. The T-100-3 can be seen operating in the endurance test facility in Fig. 3.

## PROCEDURE

The T-100-3 discharge and cathode #/1 were purged with xenon when the mechanical pumps were used to pump the vacuum tank from atmosphere to 50 mTorr. The T-1003 was operated only if the vacuum tank base pressure was below  $2.7 \times 10^{-5}$  Pa ( $2 \times 10^{-7}$  Torr). During a facility shutdown (cryopumps off) the T-100-3 was purged with xenon. The thruster was turned on by energizing the discharge supply and igniting the cathode. Cathode igniter voltage was set at 250 V; if the cathode did not start at this voltage the ignitor supply voltage was increased until cathode ignition occurred.

An operating cycle was defined as any time the thruster achieved a discharge current of  $>1.5$  A. The first 35 cycles of the wear test were used to evaluate the performance of two different T-100-3 thrusters, test the data acquisition and control program, the vacuum facility, and the probe rake. In these cycles the thruster were operated for varying time periods, from less than one minute to over 60 minutes, and at varying discharge currents and discharge voltages.

Discharge voltage was measured between the anode and cathode emitter, at the vacuum tank feed through. Discharge current and magnet current were measured across calibrated current shunts and through

current meters. Magnet voltage was measured across the magnetic coils at the feed-through. Floating voltage, measured between the cathode emitter and facility ground, and thruster body voltage (defined as the potential between the thruster body and facility ground) were measured at the vacuum tank feedthrough. The computer data for thruster currents and voltages were calibrated and compared to data taken at the vacuum tank feed-through with hand-held voltmeters throughout the wear test.

During wear test cycles the computer performed the task of removing power to the thruster, taking/storing thruster and system data, and monitoring the facility. At the beginning of every cycle the flow meter voltage with no flow was measured. Oscilloscope traces of the discharge current and discharge voltage were obtained roughly two times every cycle. Approximately every 100 hours the life test was interrupted for a short period of time to photograph the thruster, perform flow rate calibrations and to re-calibrate the thrust stand. 11 thrust stand calibrations and 6 flow rate calibrations were performed during and at the completion of the wear test.

Thruster start-up procedure was as follows: thruster discharge flow was set to 4.7 mg/sec and the cathode flow to 2 mg/sec. Discharge voltage was set to 300 V on the discharge power supply, and cathode ignitor voltage was preset to 250 V. Computer storage frequency was set to every three seconds. The igniter supply was turned on, which normally resulted in cathode ignition and thruster start. If the cathode did not start the cathode ignitor voltage was increased until cathode ignition was achieved. After thruster start the cathode flow rate was re-adjusted to its nominal value of 0.37 mg/sec.

## RESULTS AND DISCUSSION

### I. Preliminary Evaluation Of T-100-3

Two different T-100-3 thrusters, dc. signaled #10 and #11, were characterized. Both of the T-100-3 thrusters were tested at NISTP for approximately 20 hours prior to being shipped to JPL. A summary of the performance characteristics of these two thrusters is shown in Table 1. Efficiency calculations include cathode, mass flow rate and magnetic coil power.

### II. WEAR TEST DATA

#### A. Wear Test Significant Events

A summary of significant events that occurred during the wear test is shown in Table 2. Cycle number vs. operating hours for thruster #11 are plotted in Fig. 4. The T-100-3 (#11) completed 49 starts and 632 hours of operation over the duration of the wear test. There were no shutdowns required due to abnormal thruster operation.

A total of 35 cycles were operated at various time intervals to test the thruster or DAC system. During the

wear test four shutdowns were commanded by the computer due to power grid surges, or to some aspect of thruster operation, such as floating voltage, that exceeded its operational limit.

A laboratory power supply was used to start the cathode. The NIITP hollow cathodes provided with the thruster do not have a tip heater for pre-heating and cathode conditioning, rather the cathodes are started at room temperature. Initially cathode #1 could be started using the laboratory power supply at 250 VDC, however by cycle 41 the cathode could not be started reliably even at 500 WC, and greater voltages (up to 1000 VDC) were required for start. It should be pointed out that a cathode ignitor built by SPI, Inc. that provides pulsed high voltage (in excess of 1,000 V) to the ignitor never failed to start the cathode. The SPI igniter supply was not available to JPL during the T-100-3 evaluation program.

The variation in discharge current as a function of time for cycle 56 is shown in Fig. 5. In wear test cycles prior to cycle 37 discharge current was approximately constant during the first 30 minutes after start. However, by the beginning of cycle 37 it was observed that discharge current increased substantially, up to 6 A, then decreased, even though the main flow rate was unchanged. This effect increased to a maximum during cycle 50, then the magnitude of increase in the discharge current began to decrease. By the end of the wear test the discharge current only increased by 1.4 A before reducing again to 4.5 A.

Also shown in Fig. 5 are thermocouple data for the thruster body, plate center and plate corner, with the thruster radiating to the facility walls that were at a temperature of approximately 23 degrees C. In the wear test the thruster was connected to a large radiator plate; both the plate and thruster were electrically and thermally isolated from the thruster stand with ceramic stand-offs. The data indicate that at a discharge of 300 V and 4.5 A the thruster reaches a steady-state temperature of 230 degrees C approximately 2.75 hours after the thruster is started. Temperature profiles after thruster shutdown are shown in Fig. 6. The data indicate that if the thruster radiates to approximately 300 K the thruster temperature approaches facility temperature in approximately 2.75 hours.

## B. Test Data For Cycles 36-69

Computer data for T-100-3 efficiency, discharge current and voltage, thrust and specific impulse for cycles 26-69 are shown in Figs. 7-12. The data were measured near the end of each wear test cycle. Thruster data were analyzed to determine cycle-to-cycle changes in thruster operating characteristics. Thrust was determined by subtracting the LVDT voltage immediately after the T-100-3 was turned off from the LVDT voltage obtained from averaging the LVDT voltage over the last two minutes of the cycle, and multiplying by the appropriate thrust stand calibration factor. To this thrust measurement was added a thrust value calculated as discussed in the Apparatus section of this paper.

Efficiency and specific impulse were calculated using the values for thrust, total mass flow rate, and engine power (including magnet power), averaged over the last two minutes of the cycle. The discharge flow rate data were not corrected for backflow.

Discharge current, discharge flow rate, and cathode flow rate are plotted as a function of thruster operating hours in Figs. 7-8. The data indicate that the flow rate required for a discharge current of approximately 4.5 A increased over the course of the wear test, from 4.77 mg/s to 4.97 mg/s; the change in discharge flow rate for a fixed discharge current occurred in the first 200 hours of thruster operation.

The T-10(-3) cathode emitter was floated with respect to the vacuum facility and was isolated from the thruster body. The thruster body was electrically isolated from the thrust stand and the cathode emitter. Floating potential and thruster body voltage are plotted as a function of thruster operating hours in Fig. 9. Floating voltage increased with operating hours to a value of approximately -14.0 V until approximately 339 hours into the wear test, then decreased to -13.3 V with 534 hours of thruster operation. The floating voltage then began to increase, but decreased after 600 hours, then again increased.

Floating voltage and thruster efficiency are plotted as a function of thruster operating hours in Fig. 10. The thruster efficiency slowly decreased until 439.4 hours, where the efficiency decreased significantly. Thruster efficiency then increased along with floating potential until 600 hours, where the floating potential decreased but thruster efficiency remained essentially unchanged.

Thrust and floating potential are plotted as a function of thruster operating hours in Fig. 11. There is a correlation between thrust and floating potential similar to that noted for efficiency and floating potential. The data indicate that the thrust remained approximately constant until 439.4 hours, where the thrust decreased significantly over a period of approximately 100 hours. The thrust decrease tracks with decreasing floating potential until after 600 hours of thruster operation, whereupon the thrust increased, possibly because of increased discharge current. With 650 hours of thruster operation the thrust and efficiency of the T-1 W-3 are similar to values obtained from the SPT-100 [30] and the NIITP T-100 wear test [28]. After approximately 600 hours of wear testing at NIITP thrust was measured to be approximately 81.5 mN [28].

Thrust and efficiency are plotted as a function of thruster operating hours in Fig. Efficiency tracks very well with the floating voltage. No explanation can be given at present to describe the changes in thruster efficiency that were observed in the wear test.

Steady-state thruster body, plate center and plate corner thermocouple data for all cycles is plotted in Fig.

13. The large decrease in thruster body temperature at 76.7 hours of thruster operation was due to a short operating time (0.35 hours) because of insufficient discharge flow rate. The thruster body temperature was approximately 230 degrees C for the duration of the test, with a slight decrease to approximately 227 degrees C near the end of the test. The radiator plate temperatures were approximately 125 degrees C at the completion of the wear test.

### C. Plume Characteristics

The current density measured by the center probe of the probe rake for two different cycles, cycle 36 and cycle 69, are compared in Fig. 14 and Fig. 15. The distance between the probe and the downstream face of the 1'-100-3 was approximately 114 cm, similar to the distance between the probe and the SPT-100 [30]. The probe was covered with plasma-spray-coated tungsten to reduce the secondary electron emission coefficient [30].

There appears to be little change in the shape of the exhaust plume over 624.4 hours, except that the peak current density at cycle 69 decreased, relative to the current density near the start of the wear test. A magnified view of the peak current densities for cycle 36 and cycle 69 are shown in Fig. 15. The plume divergence angle, defined as the plume full width at half maximum, is approximately 16 degrees. The plume data for the 1'-100-3 are very similar to plume data from cycle 863 (hour 640) of the SPT-100 wear test [30, 34]. The full width at half maximum for the SPT-100 with 640 hours of thruster operation was approximately 16 degrees.

#### 1). Post-Wear Test Inspection

After the completion of the wear test (cycle 69) the vacuum chamber was opened and the thruster was examined and photographed. The wear data described in sections D. 1 and D.2 below were obtained from the physical inspection performed after the vacuum chamber had been opened.

#### D.1. Insulator Erosion

Erosion of the discharge chamber insulator surfaces was documented photographically. Erosion data are depicted schematically in Fig. 16. The data indicate that the inner insulator wear rate was about a factor of three lower compared to the WT-100 [18], and the outer insulator wear rate was similar to the SPT-100 except diagonally across the electromagnets, where the T-100-3 wear rate was approximately 30% greater than the wear rate for the SPT-100. NIITP observed similar insulator wear rates in their 2,000-hr wear test [28]. However, since the T-100-3 outer insulator is thicker than the SPT-100 insulator, 1'-100-3 operating life due to insulator erosion should be comparable to the SPT-100 if life time estimates are based on insulator wear rates.

#### 1).2. Cathode Erosion

Cathode erosion is represented in the schematic diagrams in Fig. 17. The outer portion of the unused cathode igniter did not appear to erode substantially. In 632 hours of operation the inner diameter of the unused ignitor cover increased by 1 mm, from 12 mm to 13 mm,

The used cathode ignitor cover OD decreased, from 21 mm to 19.7 mm. Molybdenum eroded from the igniter was found deposited on areas of the thruster body that faced the used cathode. The inner diameter of the used igniter increased by 1 mm, from 12 mm to 13 mm. The thickness of the igniter cover decreased, from 4.8 mm new to 4.3 mm at the end of the wear test. It is likely that the first failure mechanism for the T-100-3 will be cathode ignitor erosion, in which the igniter erodes too much for proper cathode ignition, deposits from the igniter contaminate the cathode emitter, or a short circuit develops between the igniter and the cathode emitter.

#### D.2. Thruster Mass Loss

Thruster mass at the beginning of the wear test was 3.525 Kg, and after 632 hours of testing the 1'-10(-3) #11 thruster weighed 3,505 Kg. Total mass loss during the wear test was approximately 20 g.

### II. Post-Wear Test Thruster Evaluation

After the thruster was examined and photographed the vacuum chamber was closed and pumped down and additional thruster performance characterization was performed. Following this, the vacuum chamber was opened, and the thruster was packaged and hand-carried to NASA LeRC to compare performance measured there with the performance measured at JPL. The data for the last wear test cycle (cycle 69), performance characterizations at JPL made after completion of the wear test and after the vacuum chamber had been opened, and performance measured at LeRC are shown in Fig. 18. The data indicate that thruster efficiency and specific impulse, measured at JPL after the vacuum chamber was opened following the WC-M test, was essentially unchanged. Efficiency and Isp measured at JPL, after completion of the wear test 0.453 and 1560 s respectively. Measurements at LeRC for efficiency and specific impulse were slightly higher than the measured efficiency and Isp at JPL; efficiency was approximately 0.465 and specific impulse was 1575 s. However, performance measurements at JPL and LeRC are very similar considering the uncertainty in the thrust and mass flow, and differences in laboratory test set-up.

#### 111. Xenon Flow Control Unit (XFCU) Tests

##### A. Description of the XFCU

The purpose of the xenon flow control unit (XFCU) is to maintain the proper xenon flow rate to the 1'-100 thruster. In order to maintain a certain discharge current at a given applied voltage, the anode flow rate has

to be maintained at a certain value. This is accomplished by using a thermo-throttle. Adding heat to the xenon flow by resistively heating part of the xenon tubing changes the viscosity of the xenon. The viscosity of xenon increases with increasing temperature of the gas, which is contrary to the behavior of many liquids. Higher heat loads produced by higher thermo-throttle currents increase the viscosity and consequently, for a given feed pressure, (in the following also referred to as plenum pressure), decrease the flow rate. Conversely, reducing the throttle current and thus the heat load to the xenon increases the flow rate.

The flow control unit used for the RHETT-1 program was built by NIITP. The unit features redundant flow paths to control each of the anode (or main discharge), cathode and cathode start-up flows. At the design inlet pressure to the XFCU of  $2.02 \times 10^5$  Pa (2 atm) the respective flow rates were to be maintained at 4.5 mg/s of xenon to the main discharge, 0.3 - 0.4 mg/s to the cathode and 1.6 mg/s through the cathode start-up line. The higher flow to the cathode is required to start the heaterless hollow-cathode.

Flow control is achieved through a series of solenoid valves, passive flow restrictors and active thermo throttles. All flow control devices, including the redundant flow paths, are placed into an approximately 64 mm wide, 54 mm tall and 195 mm long housing. The entire assembly (excluding electrical connectors) weighs 557.8 gram. Adding the weight of the electrical connectors increases the weight to 586.8 gram. The unit features a single propellant inlet. The tubing (inlet and outlet) is specified at 2 mm OD and was measured at 1.98-1.99 mm OD. The tubing wall thickness is roughly 0.5 mm. A 3 mm OD end stub features metric Russian fittings similar to the S wagelok® fittings known in the WCSL. The...c fittings feature an internal M8x1 thread. The tubing is made from a Russian steel containing 12% Cr, 18% Ni and 9 %Ti..

The flow schematic of the XFCU is shown in Fig. 19. The inlet tubing leads to a pair of solenoid isolation valves via a tee-joint that splits the flow path into the two redundant branches. In the following, these branches will be referred to as A1/K 1 and A2/K2, using the NIITP notation. The solenoid valves could not be weighed individually since they were received at JPL, assembled into the XFCU. However, NIITP data indicate a weight of 35 gram per valve. The valves require a voltage of 27 Vdc to open, however, as will be shown below, tests revealed that the valves are able to open at significantly lower voltages, down to 15 Vdc.

Following the isolation valves, within each branch, A1/K 1 and A2/K2, the flow path splits up further into anode (main discharge), cathode and cathode-start-up paths. Each path features a solenoid valve identical to the type used for the isolation valves. Following the valves is an active thermo-throttle in the case of the anode, flow path, and passive flow restrictors in case of the cathode and cathode start-up paths. Within the thermo-throttle

itself the flow path is split up further into three parallel tubing segments about 2-3 cm in length. Diameters of these tubing segments were not measured, however, the ODs are significantly smaller than the 2mm inlet tubing. Current passed through the walls of these three tubing segment heats the xenon flow. By splitting up the flow into those three parallel, narrower flow passages, better heat transfer to the xenon flow and a flow restriction effect is achieved. The flow restrictors in the cathode and cathode start-up branches consist of appropriate lengths of small diameter tubing (not measured) wound into coils to accomplish the necessary flow reduction. The anode path then connects to an outlet tubing of the, same dimensions as the inlet tubing. Cathode and cathode start-up flows are first joined via a tee-connection and then also connect to the same size outlet tubing as the inlet. Given the two redundant branches A1/K 1 and A2/K2, the flow control unit thus features four outlets (2 anode and 2 cathode outlets) and one central inlet.

A four pin Russian-built electrical connector provides the electrical interface to the two thermo-throttles of the unit and a ten-pin connector provides the interfaces for the eight solenoid valves. Eight negative lines and two positive lines connected to all eight valves with one serving for redundancy make up the ten-pin connector. Throttle resistances were measured at the connector as  $0.20 \Omega$  for the throttle of branch A1/K 1 and  $0.21 \Omega$  for the A2/K2 throttle.

## B. Test Set-up and Procedure

The XFCU was installed in the 3m dia., cryopumped vacuum chamber already described earlier. The unit was placed near the thrust stand, roughly 35 cm away. The XFCU was connected to a propellant feed system located in a control room adjacent to the vacuum chamber, separated from the tank by roughly 8 m of 1/4 inch (6.35 mm) tubing. The feed system, shown in Fig. 20, was originally designed for ion engine operation and thus features main, cathode and neutralizer ports. The XFCU inlet was connected to the pump out line, originally used to pump out the feed system via the vacuum tank and its pumping facilities. The flow system was modified from its use in the XFCU tests by installing an additional flow meter into the line, connecting the feed system to the xenon supply. The redundant anode and cathode XFCU outlets, respectively, were joined prior to being connected to the anode inlet and one of the two thruster cathodes of the T-100. During another set of tests, aimed at determining leak rates through XFCU valves, the anode and cathode outlets of the unit were again joined, but subsequently connected to the main and cathode ports of the feed system shown in Fig. 20, respectively. Pressure gages mounted to the main and cathode calibration ports shown in Fig. 20 were able to measure pressure rise and allow determination of valve internal leak rates.

Some of the tests performed with the XFCU required operation of the unit at lower than room



temperatures. For these tests, the XFCU was placed on a copper cold plate. A Glycol bath located outside the vacuum chamber was cooled by two cold fingers connected to one cooler each. A pump circulated the glycol via a vacuum feed through to the copper cold plate. The XFCU was further shielded by MLJ blankets wrapped around the unit to protect it from heat radiation from the surrounding vacuum tank, which was at ambient temperature. Temperature sensors located on the XFCU and the cold plate recorded the temperature values. This set-up allowed temperatures as low as 2.6 C at the XFCU at beginning of operation, before the unit started warming due to heat dissipated in the opened valves and the thermo-throttles. The corresponding temperature of the cold plate at this point of operation was -1.2 C.

Two DC power supplies provided the necessary power for valve actuation and the thermo-throttles. A simple switch board was used to independently open and close the various XFCU solenoid valves. Due to the physical separation of the control room and the vacuum chamber, roughly 8 m of 20 gage wire was used to connect the power supplies to the XFCU. The resistance of the wiring was measured at 0.6 -0.7  $\Omega$  which added to the roughly 0.2  $\Omega$  of throttle resistance.

## C. Results

### XFCU Acceptance Tests

During the first set of tests, the XFCU, although connected to the thruster, was operated with the thruster off. These measurements focused on the determination of the flow rates through the various flow paths through the unit, and their dependence on throttle current, XFCU inlet (plenum) pressure and ambient temperature. Performing these tests without simultaneous thruster operation simplified the conduction of these tests and allowed a wider range of the XFCU performance parameters to be tested.

Figure 21 shows the pressure dependence of various flows and combination of flows through branch A1/K1 of the unit. These data indicate that for the specified inlet (plenum) pressure of 0.202 MPa (29.2 psia), the anode flow rate is around 7.6 mg/s and the cathode flow rate is almost 0.7 mg/s (compared to the required values of about 5 mg/s and 0.3 - 0.4 mg/s, respectively). The cathode flow rate was found to be too high for operation at the design XFCU inlet pressure. Ideal cathode flow rates for the T-100 thruster at nominal operating conditions are 0.3 -0.4 mg/s. Similarly, the anode flow rate was found too high. Anode flow rates required to maintain the discharge current at its desired value of 4.5 A usually are found around 4.8 -5.0 mg/s. This problem was subsequently corrected in future XFCU units built at NIITP by appropriately sizing the length of tubing acting as flow restrictors in the respective lines of the XFCU.

In the case of the anode flow, however, a sufficiently high throttle current is able to lower the anode

flow rate to the desired values even at the 0.202 MPa inlet pressure value. As shown in Fig. 22, a throttle current slightly greater than 2.5 A is required at the design pressure to maintain the correct anode flow rate. The design value for the throttle current at the nominal operating condition was originally specified at approximately 1.5 A. For a throttle current of 1.5 A, Fig. 22 shows that the inlet pressure to the XFCU would have to be lowered to around 0.172 MPa (25 psia) for this unit.

Figure 23 shows the behavior of cathode flow vs. inlet (plenum) pressure for OA throttle current and for the required value for nominal operating conditions of the thruster (2.5 A). Note that the thermo-throttle does not act directly on the cathode flow since it is placed only in the anode flow lines. As Fig. 23 shows, the cathode flow tends to drop slightly at higher throttle currents. This can likely be attributed to a warming-up effect of the XFCU unit due to heat dissipation in the throttle. This effect, however, is significant at the 0.202 MPa design operating condition of the unit and is around a 0.1 mg/s reduction in flow. It is unclear what this value would be for a redesigned unit which delivers 0.3 -0.4 mg/s cathode flow at 0.202 MPa inlet pressure.

Another interesting and so far unexplained phenomenon was noted when comparing the combined anode and cathode flow measured at 2.5 A throttle current with the individually measured flow rates for anode and cathode. As Fig. 26 shows, the cathode flow rate that has been computed by subtracting the measured anode flow rate at 2.5 A throttle current from the corresponding measured combined anode and cathode flow rates is larger than the measured cathode flow rate when the throttle current was set to 2.5 A. This behavior was found to be repeatable. One possible explanation is that a leak developed somewhere in the cathode flow line at elevated temperatures caused by the thermo-throttle. This explanation, however, is purely speculative at this point. It should be noted, however, that no discrepancy was found between these flow rates at OA throttle current as Fig. 21 demonstrates. The corresponding flow rates, calculated from the curve fits to the data of Fig. 21 are listed in Table III and, as can be seen, add up almost perfectly. Small remaining differences may be real or may be attributed to inaccuracies in the flow measurement.

The temperature sensitivity of the various flow rates was investigated further by cooling the XFCU as described above and operating the unit at various temperatures ranging from 2.6 C to 32 C. Figures 24 and 25 show the results for the anode and cathode flows of branch A1/K1. Similar results were obtained for the corresponding flows of branch A2/K2. The curve featuring solid symbols were taken at a previous test run. For each curve a temperature range is given because XFCU temperatures changed rapidly during the data recording as heat dissipated by the opened solenoid valves raised the XFCU temperature. The cooling loop set-up described above was not able to maintain the XFCU at the low temperature when the XFCU was operating.



According to the curve fits given in Fig. 24, anode flow rates drop from 8.8 mg/s to 7.6 mg/s as the temperature increases from about 2-4 °C to 30-32°C at 0.202 MPa (29.2 psia) inlet pressure, corresponding to a 13 % drop in flow rate or about 0.04 mg/s per degree C. At lower pressures the corresponding flow rate differences are 14% or 0.03 mg/s per degree C at 0.172 MPa (25 psia) and 16% or 0.02 mg/s per degree C at 0.138 MPa (20 psia). These are sizable mass flow rate changes that will have to be taken into account when designing the thermal-control subsystem for a flight unit.

As can be seen in Fig. 25, cathode flow rates do not seem to vary as predictably with temperature as anode flow rates do. This may be a real effect or, more likely, may be due to the increased difficulty of measuring the much smaller cathode flow rates with the same relative accuracy as the larger anode flow rates. Nonetheless, the same trend as observed for the anode flow rates is also visible in Fig. 25 in that flow rates drop as temperature of the XFCU increases. Here, at 0.202 MPa (29.2 psia or 2 atm) inlet pressure, the cathode flow rate drops from 0.76 mg/s to 0.7 mg/s or by 8%, corresponding to a flow rate drop of about 0.002 mg/s per degree C. At 0.172 MPa (25 psia) inlet pressure the corresponding flow rate drop is 9.7 % or 0.002 mg/s per degree C and at 0.138 MPa (20 psia) this drop is found to be 9.7 % or 0.001 mg/s per degree C. Although the cathode flow rates are too high at the design XFCU inlet pressure for this particular unit as was pointed out before, the cathode flow rate changes appear acceptable.

Finally, flow rate transients were measured to determine the time it takes to complete the flow rate changes when turning the thermo-throttle on or off. Here the thermo-throttle current was set to 2.5 A to operate this particular XFCU unit at the required anode flow rate of about 5 mg/s. Figure 26 indicates that the desired flow rate can be achieved within about three minutes after turning the throttle on. Similarly, it takes about three minutes to return the flow rate to its original cold flow condition when the throttle is turned off, as shown in Fig. 27.

## XFCU/T-100 integration Tests

Following the tests without thruster operation, the XFC unit was tested with the T-100 operating. Here, of particular interest were the impact of throttle current on discharge current via mass flow rate changes and temperature effects on the XFCU and their influence on thruster performance.

Figure 31 shows the relationship between discharge current and throttle current. As can be seen, roughly 2.5-2.6 A throttle current are required to maintain the desired beam current of 4.5 A for this particular XFC unit which is consistent with the value determined by measuring the anode flow rate sensitivity to throttle current as discussed above. A change in throttle current of 1 A will effect a change in discharge current of about 1.5

A for an inlet pressure of 0.202 MPa (29.2 psia). At about 0.172 MPa (25 psia), the effect changes in throttle current have on beam current are less pronounced. Here, a 1 A change in throttle current only results in a 1.2 A change in beam current. As Fig. 29 indicates, the change in discharge current is entirely due to a change in mass flow rate, since the slopes of both mass flow rate, and discharge current curves are virtually identical, in particular for the case of 0.202 MPa (29.2 psia) pressure where the impact of the almost constant cathode flow rate on total flow rate is less pronounced (the slopes can easily be taken from the mathematical curve fit expressions listed in Fig. 29).

Figure 33 shows how much electrical power is required to maintain the required mass flow rates. As can be seen, about 5.5 W are required to maintain the correct discharge flow with this XFC unit. It should be pointed out, however, that the long wiring required to connect the XFCU to the power supplies in this set-up significantly increased the power requirements. Resistance of the XFCU throttle circuit increased by about 0.7 Ω due to the longer wire. If power supplies could be placed closer to the XFCU, eliminating long wiring, these power requirements may be reduced to almost 20% of the measured value in this set-up, or about 1.2 Watt. This value is very small in comparison to the power dissipated in the thruster and demonstrates a highly efficient design. Note also, that this particular XFCU required higher throttle currents than usual to maintain the correct flow at the specified design pressure of 0.202 MPa (2 atm). If flow restrictors and thermo-throttles were, redesigned resulting in lower throttle currents, the throttle power requirements could be reduced further by a significant amount. If by proper design of the flow restrictors and throttles the throttle current could be lower to the original design value, of 1.5 A, power requirements would further drop by almost a factor of three, or to about 0.4 - 0.5 Watt.

As with the XFC unit alone, temperature sensitivity tests were performed during the integrated XFCU/T-100 tests. In the tests described in the following paragraphs, only the XFCU was cooled while the T-100 allowed to operate at its usual operating temperature when placed in a room temperature environment (typically around 230 °C). Using this approach, temperature effects on the XFCU could be easily isolated. Figure 28 shows the impact on thruster operation as expressed by the discharge current. Since elevated XFCU temperature and throttle current both increase xenon viscosity, thus lower xenon flow, less throttle current is required at elevated XFCU temperatures to maintain the T-100 nominal flow condition. For 4.5 A beam current, the throttle current can be reduced by 0.3 A from 2.9 A at 14 °C to 2.6 A at 32 °C. At higher beam currents of 4.9 A the change is 0.3 A also from 2.6 A to 2.3 A. At a lower beam current of 4.1 A the change is 0.4 A from 3.2 A at 14 °C to 2.8 A at 32 °C. As mentioned, these temperature effects are fairly sizable and should be taken into account when designing the thermal control subsystem for the XFCU/T-100 flight environment.

Figure 32 shows the changes in total mass flow rate for varying throttle currents and the two different temperature conditions. Again, slopes for the beam currents of Fig. 31 and for the mass flow rate of Fig. 32 are virtually identical, demonstrating that changes in beam current with throttle current result from changes in total mass flow rate.

#### **IV. Xenon Propellant Storage and Distribution System (PSDS) Evaluation**

##### **A. Description of PSDS and Components**

The purpose of the PSDS is to feed propellant from a propellant tank into the XFCU at the appropriate flow rate and XFCU inlet pressure. The PSDS underwent many design reviews to fit the changing needs of the RHETT-1 system, some occurring late in the program. The propellant tank was eliminated fairly early from the system since it is highly mission specific and the demonstration of pressurized xenon storage was not believed to be a necessary part of the RHETT-1 program which sought to demonstrate a "flight-type" Hall electric thruster system. The remaining system finally took on the form shown in Fig. 33. A schematic of the system is shown in Fig. 34. The system was provided by Moog Space Products.

The final design iteration consisted of a latch valve by Moog serving as the isolation valve of the system, a one-stage regulator, also by Moog, able to regulate xenon from an inlet pressure of 9.307 MPa (1350 psia) to an outlet pressure, set by the desired XFCU inlet pressure, of about 0.202 MPa (29 psia). The system featured two pressure transducers (high and low) by Paine, located upstream and downstream of the regulator and two fill and drain valves, again by Moog. In the last design iteration of the PSDS shown in Fig. 33, one of the fill and drain valves is used in the unusual function as the inlet to the system. Typically, inlets to propellant feed systems use welded joints, or, in the case of a laboratory model such as the system described here, use Swagelok® or AN fittings. However, at the time the last design change to the PSDS was made, the fill and drain valves were already built and thus were used in the function described. The PSDS is mounted together with the XFCU on an aluminum mounting plate. The overall weight of the system components (excluding the XFCU and mounting plate) is 996 gram.

The latch valve is based on an earlier design by Moog Space Products for the Pluto Fast Flyby program and was modified for operation at higher pressures. The Maximum Expected Operating Pressure (MEOP) is 14.996 MPa (2175 psia) and the unit was proofed to 22.683 MPa (3290 psia). The latch valve weighs 112 gram and features an internal propellant filter with an absolute filter rating of 5 micron. The valve has an

transducer installed both upstream and downstream of the mass flow meter.

### C. Results

The results of the pressure regulation tests are shown in Table IV. As can be seen the pressure just upstream of the mass flow meter installed external to the PSDS, is within 1379 Pa (0.2 psia) between 0.198 MPa (28.72 psia) and 0.199 MPa (28.95 psia) for inlet pressures ranging from around 0.069 MPa (100 psia) to 0.110 MPa (741.2 psia, max. xenon bottle pressure). The original specification for the Moog regulator required the pressure to be maintained at  $29 \pm 1.0$  psia (0.200 MPa  $\pm$  0.069 MPa) and was successfully achieved. Mass flow rates were maintained at 50.3 to 50.4 sccm of xenon throughout these tests, corresponding to xenon flow rates encountered at nominal T-100 operation. The PSDS was thus found to operate successfully and several PSDS components, including the regulator, were taken over into the RHETT-1 follow-on program, RHETT-2.

### V. PSDS, XFCU and T-100-3 integrated Tests

The xenon propellant system, xenon flow control unit and T-100-3 were installed into the vacuum chamber and tested as an integrated system. A series of tests were performed to evaluate the system and are described below. Cathode #2 was used for the tests described below; cathode #1 was unavailable. No thrust measurements were obtained. The SPI cathode ignitor power supply was used in these tests to start the cathode.

#### A. Cold Cathode Starting

Since the NIIP cathode has no tip heater, there was concern that the cathodes may not start at very cold temperatures. Experiments were performed to evaluate ignition characteristics of the NIIP hollow cathode. A shroud cooled with liquid nitrogen was placed around the thruster body so that only the downstream face of the T-100-3 faced room-temperature. The other five sides of the thruster faced the LN<sub>2</sub> shroud. The thruster was thermally isolated from the shroud. Thermocouples were attached to the pressure regulator, the T-100-3 body (side next to the cathode anti the side 180 degrees from the cathode) and to the thruster cathode near the thruster body. LN<sub>2</sub> was flowed through the shroud until the cathode thermocouples indicated that the cathode was below two degrees C, and the thruster body was below 3.5 degrees C. The XFCU was used to supply xenon to the cathode and was operated at room temperature during cold cathode ignition experiments. A laboratory propellant system was used to supply xenon to the XFCU for these tests.

The cathode, with an indicated barrel temperature of less than 2 degrees C, was ignited at a flow rate of between 0.35-2 mg/s for ten starts without incident.

Fifteen additional cathode starts were performed with the cathode flow at 2 mg/s, a cathode temperature as low as -23 degrees C and a thruster body temperature as low as -15 degrees C. The data indicate that the T-100-3 heaterless cathode, when new, can be reliably started at temperatures as low as -23 degrees C.

LN<sub>2</sub> shroud temperature as a function of time after T-100-3 start is shown in Fig. 36. Shroud temperature was initially approximately -140 degrees C (133 K) until the thruster was turned on, whereupon the shroud temperature increased to approximately 153 K. Cathode barrel temperature data are shown in Fig. 36. The data indicate that the thruster cathode barrel achieved a steady-state temperature of about 220 degrees C approximately 200 minutes after the thruster was turned on.

#### B. Cold Pressure Regulator Tests

Experiments were performed to measure PSDS pressure regulator performance as a function of regulator temperature. Thermocouples were attached to the pressure regulator and to the PSDS plate. The flow rate was controlled using the XFCU and propellant was exhausted through the thruster. Xenon feed pressure into the pressure regulator was approximately 5,540 kPa (804 PSIA). The data for this test are summarized in Fig. 37. The data indicate that with a base plate temperature of -24.8 degrees C, a regulator temperature of 21 degrees C, and a feed pressure of 803 PSIA there are no measurable variations in the regulated pressure. Some variations in regulated pressure were observed at regulator temperatures below 20 degrees C. Significant variations in regulated pressure occurred only at regulator temperatures below 5 degrees C. At a regulator temperature of 0 degrees C, variations in regulated pressure, occurred at feed pressures above 340.7 PSIA. High pressure transducer output voltage as a function of temperature is shown in Fig. 38. The pressure transducer output was stable over the temperature range tested.

#### C. Integrated System Testing

The PSDS, XFCU and T-100-3 were placed in the vacuum chamber and tested together as an integrated subsystem. First, a pressure rate-of-rise test was conducted to verify that no part of the PSDS and XFCU leaked. The pressure rate-of-rise tests were performed with the valve to the PSDS closed, the XFCU supply valves open, and the XFCU cathode/antic valves closed; leakage anywhere in the trapped volume between the supply line to the PSDS and the XFCU valves would be revealed via pressure decay in the trapped volume. At a feed pressure of 5,518.4 kPa (800.0 PSIA), a maximum leak rate of 0.008 sccm was calculated. The resolution of this test was limited by the amount of time for the pressure decay test (approximately 18 hours), and it is possible that the leak rate could be less than reported herein.

The PSDS was supplied with xenon at a regulated pressure of 5,541 kPa (804 PSIA); the PSDS

supplied xenon to the XFCU at a regulated pressure that depended on regulator temperature. At the nominal conditions of 300 V and 4.5 A and a regulator temperature above 21 degrees C the discharge flow rate and thruster discharge were stable. Regulated pressure did not vary by more than plus/minus 0.01 PSIA over the test. Once thermal equilibrium was achieved, there were no observable variations in thruster flow rate or discharge current. The XFCU worked very well with the PSDS and the T-100-3 and provided excellent discharge and cathode, flow rate control. With the XFCU controlling the engine mass flow rates a variation in the discharge current of  $\pm 7$  mA (out of a total of approximately 4.5 A) was easily achieved. After reaching thermal equilibrium it was not necessary to adjust the XFCU current settings to maintain a constant discharge current unless the feed pressure changed. The NIITP thermothrottle provides much better flow rate/discharge current control than use of micrometer valves.

Data for the integrated subsystem testing in vacuum are summarized in Table V. Subsequently the PSDS, XFCU and T-100-3 were integrated into the RHETT-1 propulsion system and tested at LERC. All subsystems performed nominally and are discussed in Ref. 26.

## CONCLUSIONS

A T-100-3 Russian Hall plasma thruster, flow control unit and US xenon propellant subsystem developed for the RHETT-1 propulsion system were evaluated for the RHETT-1 propulsion system. The thruster evaluation program included performance testing at various discharge voltage and input power levels, and a 632-hour wear test. Thrust and efficiency of the T-100-3 are comparable to the SPT-100. The endurance test was performed for 349 on/off cycles and 632.4 hours of operation at an input power to the thruster of approximately 1.35 kW. Each cycle was nominally 24 hours of thruster on-time and ten minutes of thruster off-time. Thrust and thruster efficiency decreased, from 83 mN and 49% at 1301, to 81.5 mN and 45% at the completion of the wear test. Thruster mass decreased by approximately 20 g over 630 hours. Over the course of the wear test the peak beam current density in the thruster plume measured on the thruster centerline decreased only slightly. T-100-3 plume characteristics are similar to those measured on the SPT-100. Inner insulator wear rates were a factor of three lower and outer insulator wear rates at certain locations were 30% greater than the insulator wear rates measured on the SPT-100. Life estimates for the T-100-3 based on the wear test data are consistent with life estimates of the SPT-100.

A Russian-designed and fabricated laboratory xenon flow control unit was evaluated over a range of XFCU temperatures, input pressures, and flow rates. The XFCU as tested featured a design error in that it was not able to deliver the proper flow rates at the specified inlet pressure of 0.202 MPa (2 atm). This error, however, can easily be corrected by sizing the tubing length of the flow

restrictors and thermothrottles properly and this design change has already been incorporated in the construction of further XFC units at NIITP. Apart from this, the XFCU performed very satisfactorily. The response time was relatively fast for a thermally controlled unit and mass flows could be easily and precisely controlled. A clear dependency of the various flow rates on ambient temperature was found which has to be accounted for when designing the thermal control subsystem for a flight unit.

The propellant system includes a pressure regulator, on/off valves, service valve and high/low pressure transducers, built to flight-like standards and assembled onto a mounting plate structure. The propellant system mass was 509 g. Testing of the propellant system included experiments to measure output pressure regulation variations through a temperature range of -20 through + 30 degrees C with an input pressure range of 414-6100 kPa (60-885 PSIA). The PSDS performed very well during JPL acceptance tests; all design specifications were met. The regulator performed exceptionally well, able to regulate xenon up to 9.308 MPa (1350 psia) inlet pressure to the desired outlet pressure of 0.202 MPa (29.2 psia). Its small size and weight were accomplished by using a single stage regulator design, despite the large ratio of inlet to outlet pressure.

The flight-like propellant feed system, T-100-3 thruster, and laboratory xenon flow control unit were tested together as a system in vacuum; all subsystems functioned nominally. The thruster, XFCU and XPS then were subsequently integrated into the RHETT-1 propulsion system at NASA Lewis Research Center and tested with a power processing unit and integrated structure.

## ACKNOWLEDGMENT

The authors thank Mr. Alison Owens and Mr. Robert Toomath for their efforts in support of the testing described in this paper. The authors gratefully acknowledge the support of Dr. Len Caveny, Innovative Science and Technology office of the Ballistic Missile Defense Organization, and Joe Welch of Space Power, Inc., San Jose, California.

The work described in this paper was performed by the Jet Propulsion Laboratory, California Institute of Technology, and was sponsored by the Ballistic Missile Defense Organization/Innovative Science and Technology, through an agreement with the National Aeronautics and Space Administration.

## REFERENCES

1. Larry, E.C., Meyrand, R. G., Jr., and Salz, F., "Ion Acceleration in a gyro-dominated neutral plasma--

- theory and experiment," Bull. Am. Phys. Soc. 7 441 (1962).
2. Seikel, G. R., and Reshotko, E., "Hall-current ion accelerator," Bull. Am. Phys. Soc. 7414 (1962).
3. Jones, G. S., Dotson, J., and Wilson, T., "Electro-static acceleration of neutral plasmas - momentum transfer through magnetic field," Proceedings of the Third Symposium on Advanced Propulsion Concepts (Gordon & Breach Science Publishers, Inc., New York, 1963) pp. 153-175.
4. Morozov, A. J. et al., "Plasma Accelerator with Closed Electron Drift and Extended Acceleration Zone," Soviet Physics -- Tech. Physics, Vol. 17, No. 1, July 1972.
5. Bugrova, et al., "Physical Processes and Characteristics of Stationary Plasma Thrusters with Closed Electron Drift," IEPC-91-079, October 1991.
6. Bober, A. et al., "State of Work on Electrical Thrusters in U. S. S. R.," IEPC-91-003, October 1991.
7. Artsimovich, L. A., "The Development of a Stationary Plasma Engine and its Test on Meteor Artificial Earth Satellite," Space Explorations, Vol. 12, No. 3, pp. 451-468 (1974)
8. Arkhipov, B. A. et al., "SPT Electric Propulsion System for Spacecraft Orbit Maneuvering," Paper RGC-HP-92-07, 1st Russian-German Conference on Electric Propulsion, March 1992.
9. "Summary of SPT Flight History", Craig Clauss of Atlantic Research Corporation, July 17, 1995.
10. Personal communication, Craig Clauss, July 11, 1995.
11. Brophy, J. R. et al., "Performance of the Stationary Plasma Thruster: SPT100," AIAA-92-3155, 1992.
12. Patterson, M. J. et al. "Experimental investigation of a Closed-Drift Thruster," AIAA-85-2060, 1985.
13. Day, M. et al., "SPT-100 Subsystem Qualification Status", AIAA-95-2666, July 1995.
14. Arkhipov, B. A. et al., "The Results of a 7,000-Hr SPT-100 Life Test", IEPC-95-39, Proceedings of the 24th International Electric Propulsion Conference, September 1995.
15. Dickens, J. et al., "Impact of Hall Thrusters on Communication System Noise", AIAA-95-2929, July 1995.
16. D. H. Manzella, "Stationary Plasma Thruster Plume Emissions", IEPC-93-097, Proceedings of the 23rd International Electric Propulsion Conference, September 1993.
17. T. Randolph et al., "Far-Field Plume Contamination and Sputtering of the Stationary Plasma Thruster", AIAA-94-2855, July 1994.
18. Garner, C. E. et al., "A 5,730-Hr Cyclic Endurance Test of the SPT-100", IEPC-95-179, Proceedings of the 24th International Electric Propulsion Conference, September 1995.
19. J. M. Sankovic et al., "Operating Characteristics of the Russian D-55 Thruster With Anode Layer", AIAA-94-3011, June 1994.
20. Garner, C. E., "Experimental Evaluation of Russian Anode Layer Thrusters", AIAA-94-3010, June 1994.
21. Marrese, C. et al., "Analysis of Anode Layer Thruster Guard Ring Erosion", IEPC-95-196, Proceedings of the 24th International Electric Propulsion Conference, September 1995.
22. Sankovic, J. M. et al., "Performance Evaluation of a 4.5 kW SPT Thruster", IEPC-95-30, Proceedings of the 24th International Electric Propulsion Conference, September 1995.
23. Petrosov, V. A., Vasin, A. I., and Baranov, V. I., "Investigation of a 4.5 kW High Efficiency Hall-Type T-160 Electric Thruster", IEPC-95-31, Proceedings of the 24th International Electric Propulsion Conference, September 1995.
24. Garner, C. E. et al., "Evaluation Of A 4.5-kW D-100 Thruster With Anode Layer", AIAA-96-2967, 32nd AIAA Joint Propulsion Conference, Lake Buena Vista, FL, July 1996.
25. L. H. Caveny et al., "The BMDO Electric Propulsion Flight Readiness Program", IEPC-95-132, Proceedings of the 24th International Electric Propulsion Conference, September 1995.
26. Sankovic, J. A. et al., "The BMDO Russian Hall Electric Thruster Technology (RHETT) Program", AIAA-96-2971, 32nd AIAA Joint Propulsion Conference, Lake Buena Vista, FL, July 1996.
27. Korotcev, A. S. and Petrosov, V. A., "NIITP's Activity in the Field of Electric Propulsion", IEPC-95-08, Proceedings of the 24th International Electric Propulsion Conference, September 1995.
28. Petrosov, V. A., Vasin, A. I., and Baranov, V. I., "A 2,000-Hour Lifetime Test Results of a 1.3 kW T-100 Electric Thruster", IEPC-95-41, Proceedings of the 24th

International Electric Propulsion Conference, September 1995.

29. Brukhty, V. I., Kirdyashev, K. P., and Svetlitskaya, O.E., "Electromagnetic Interference Measurements Within The T-100 Endurance Test", Proceedings of the 24th International Electric Propulsion Conference, September 1995.

30. Garner, C.E. et al., "Performance Evaluation and Life Testing of the SPT-100", IEPC-93-091, Proceedings of the 23rd International Electric Propulsion Conference, September 1993.

31. NIST calibration data reference.

32. Haag, T.W. and Curran, F. M., "Arcjet Starling Reliability: A Multistart Test on Hydrogen/Nitrogen Mixtures," AIAA-87-1061, May 1987. (NASA TM-898867).

33. Knowles, T. R., Energy Sciences Laboratories, inc., San Diego, Ca, Personal Communication, "Flocked Space Radiator", December 10, 1994.

34. NIITP reference about heated hollow cathodes.

35. Manzella, D.H. and Sankovic, J. M., "Hall Thruster Ion Beam Characterization", AIAA-95-2927, July 1995.

**Table 1. T-100-3 Performance Characteristics Measured at JPL. Data for the T-100-3 #1 1 are beginning of life (1101.),**

2'-100 Desig.	Cycles	Testing at JPL (Hrs)	Discharge Voltage (v)	Discharge Current (A)	Discharge Flow* (mg/s)	Cathode Flow (mg/s)	Magnet Power (w)	Thrust* (mN)	Thruster Efficiency*
#10	1-20	14.0	299.7	4.52	4.8	0.36	36	82.4	0.48
#11	25	7.1	300	4.49	4.77	0.35	28	81.3	0.47
#11	30	7.1	200	4.52	4.81	0.37	24	62.0	0.41
#11	35	7.1	301	4.00	4.29	0.36	18	72.6	0.46

\*Not corrected for backflow of facility xenon into the thruster

\* -1.4 mN was added to measured thrust to include cold gas thrust component, as discussed in the Apparatus section of this paper

**Table II. T-100-3 Wear test Significant Events**

Cycle	Total* Thruster Hours	Description
21-35	27.1	3'-100-3 # 11 characterization and DAC system check
36	27.1	Wear test started
37	65.6	Discharge current increases during first few minutes after start-up
38	76.4	Computer shutdown, I.VDT exceeded lower limit due to thrust stand inclination failure
39	76.4	First observation of flickering, unstable plume; manual shutdown because of insufficient discharge flow rate
41	99.0	No thruster start at 500 V, 20 mA
42	141.6	Turned off cryopumps to remove helium from facility
43	141.6	Sparks from discharge chamber on start-up
44	185.1	Changed xenon bottles
48	256.6	Ignitor supply capacitor failure, manually turned off thruster
53	360.5	Significant wear in cathode. # 1 observable
55	396.8	Computer shutdown due to power grid surge
56	416.5	Computer shutdown due to low discharge flow rate
61	534.2	No thruster start at 500 V, 20 mA; computer shutdown due to power grid surge
62	576.0	No thruster start at 500 V, 20 mA; computer shutdown due to floating potential exceeded lower limit
69	651.5	12s1 wear test cycle
70-88	665	T-100-3 characterization at JPL and LERC

\* Includes approximately 20 hours of operation at NHTP

**Table III: Comparison of XFCU Flow rates at OA Throttle Current**

Pressure (MPa)	Anode Flow (mg/s)	Cathode Flow (mg/s)	Cathode Start Flow (mg/s)	Measured Anode+Cathode (mg/s)	Measured Anode+Cathode + Cathode Start (mg/s)
0.138 (20 psia)	3.72	0.36	1.26	4.07	5.47
0.172 (25 psia)	5.82	0.52	1.79	6.36	8.15
0.202 (29.2 psia)	7.64	0.68	2.31	8.28	10.21



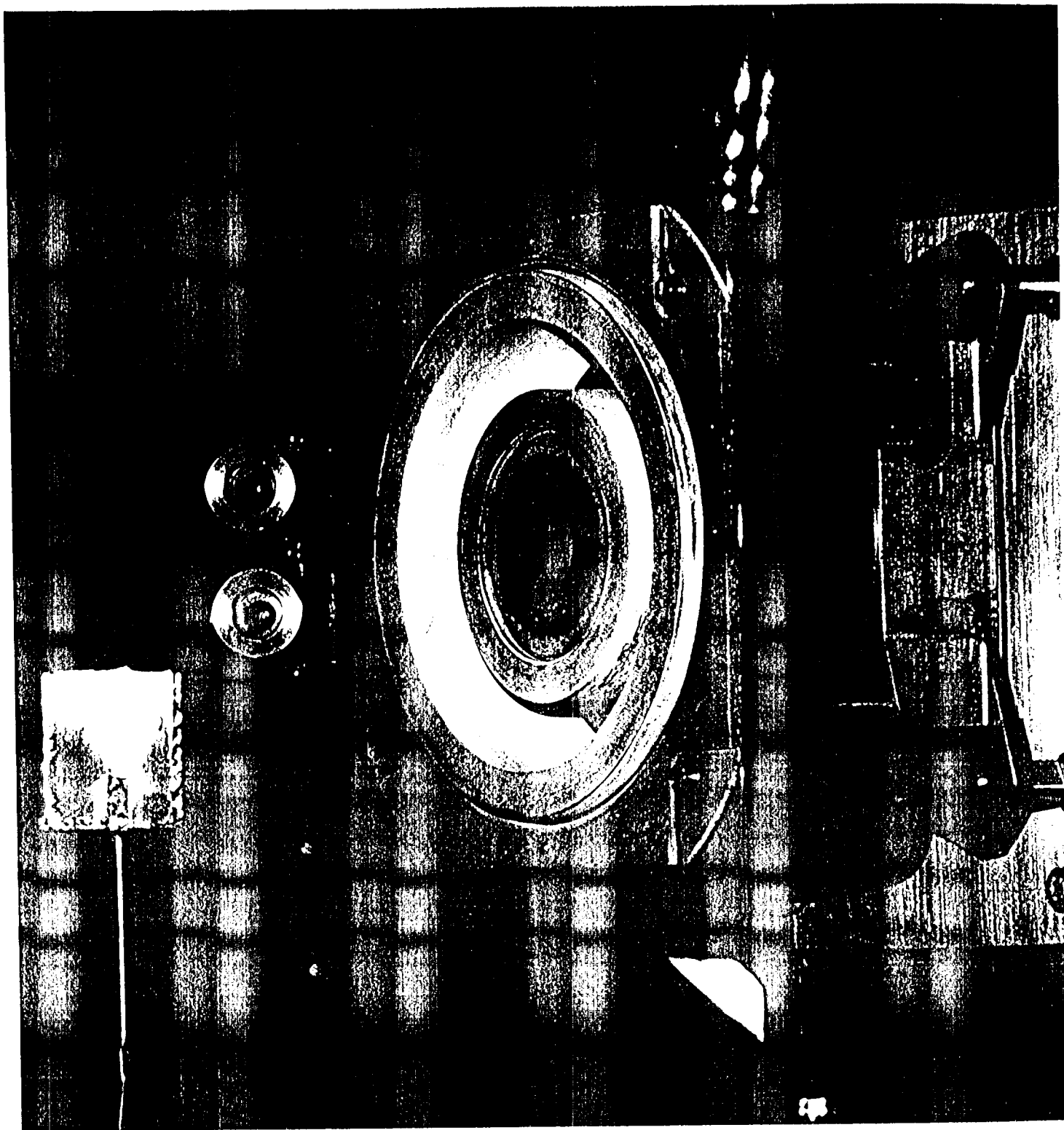
Table 1 V: Results of PSDS Acceptance Tests at JPL

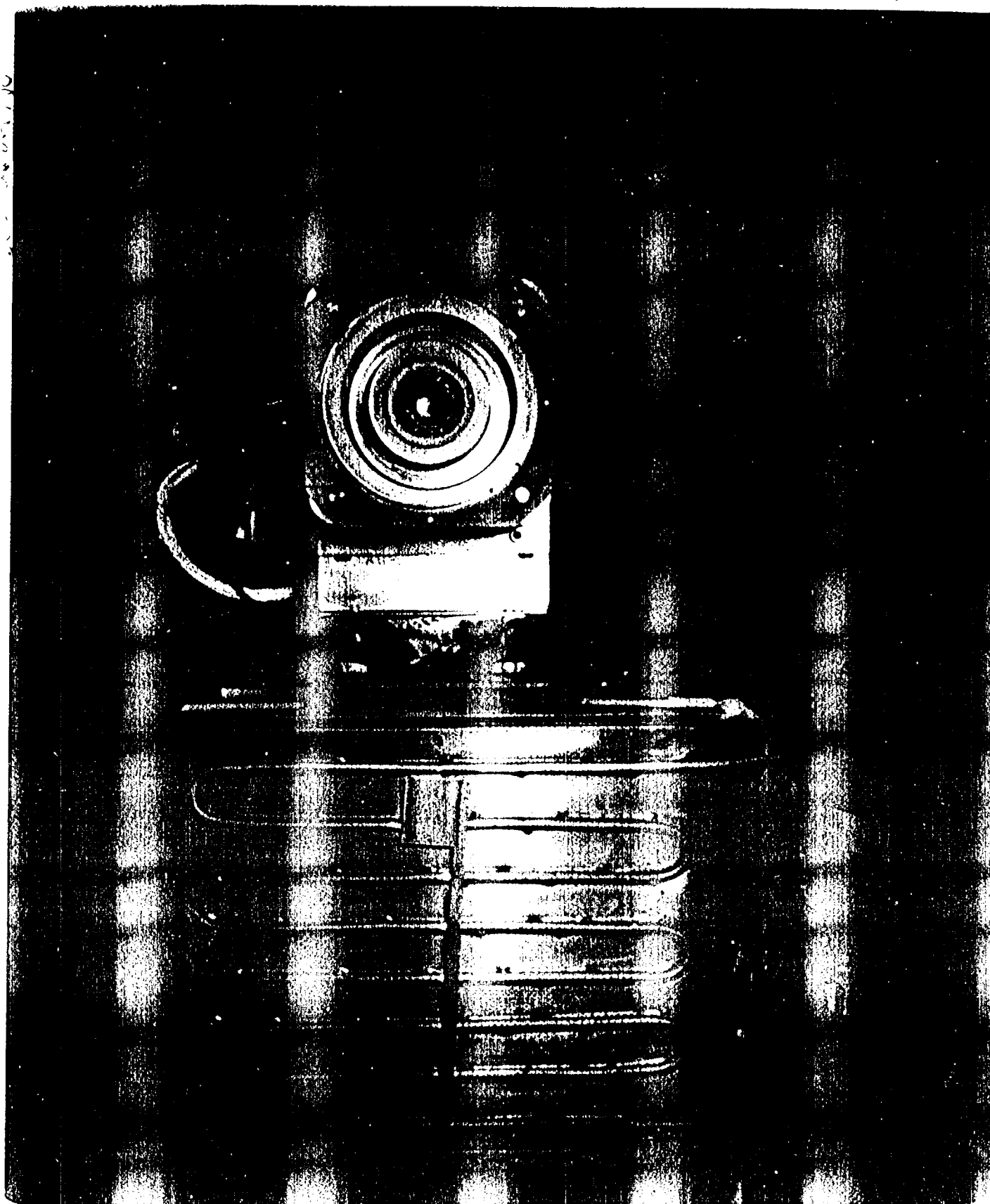
Feed Pressure	Pressure upstream of Flowmeter	Pressure Downstream of Flowmeter	PSDS Low Pressure transducer	Mass Flow Rate
(psia)	(psia)	(psia)	(psia)	(scm)
93.8 -101.1	28.72-28.73	28.33	###	50.3
32.1 .5-321.7	28.83-28.84	28.43	###	50.5
499.0-499.1	28.86-28.87	28.46	###	50.3
645.9	28.82	28.52	###	50.4
646.2	28.82	28.52	###	50.4
741.2	28.95	28.54	###	50.4

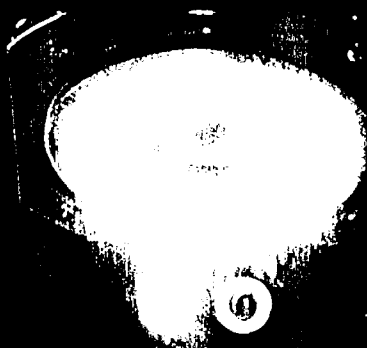
Table V. Integrated Test Data

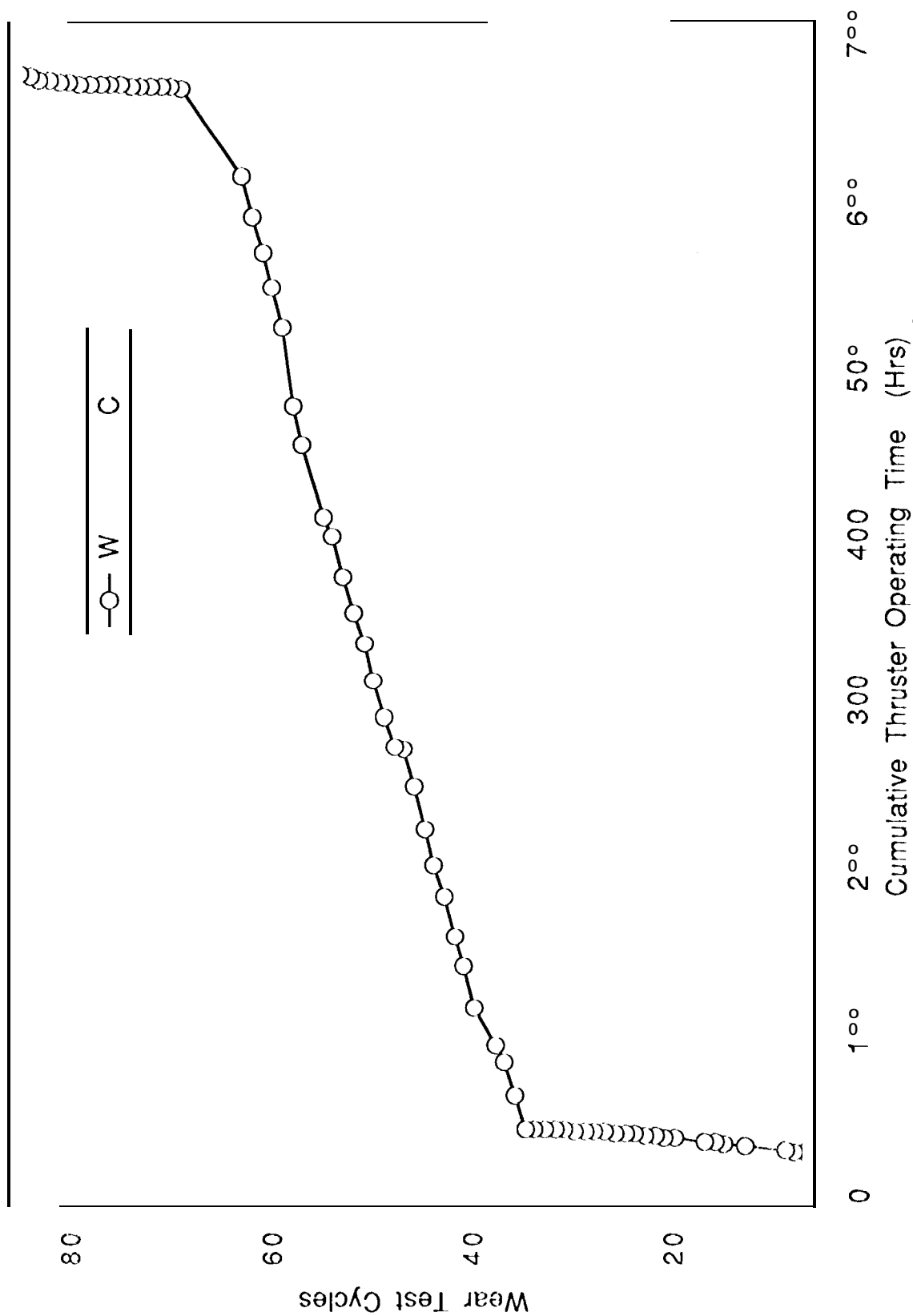
Thruster Voltage (V)	Discharge Current (A)	Total Flow Rate (mg/s)	Regulated Pressure psia)	Pressure (V)*	Thermosthrottle (A)	(V)
297.5	4.49	5.7	28,7	1.43	2.0	2.35

\* Pressure regulator output voltage







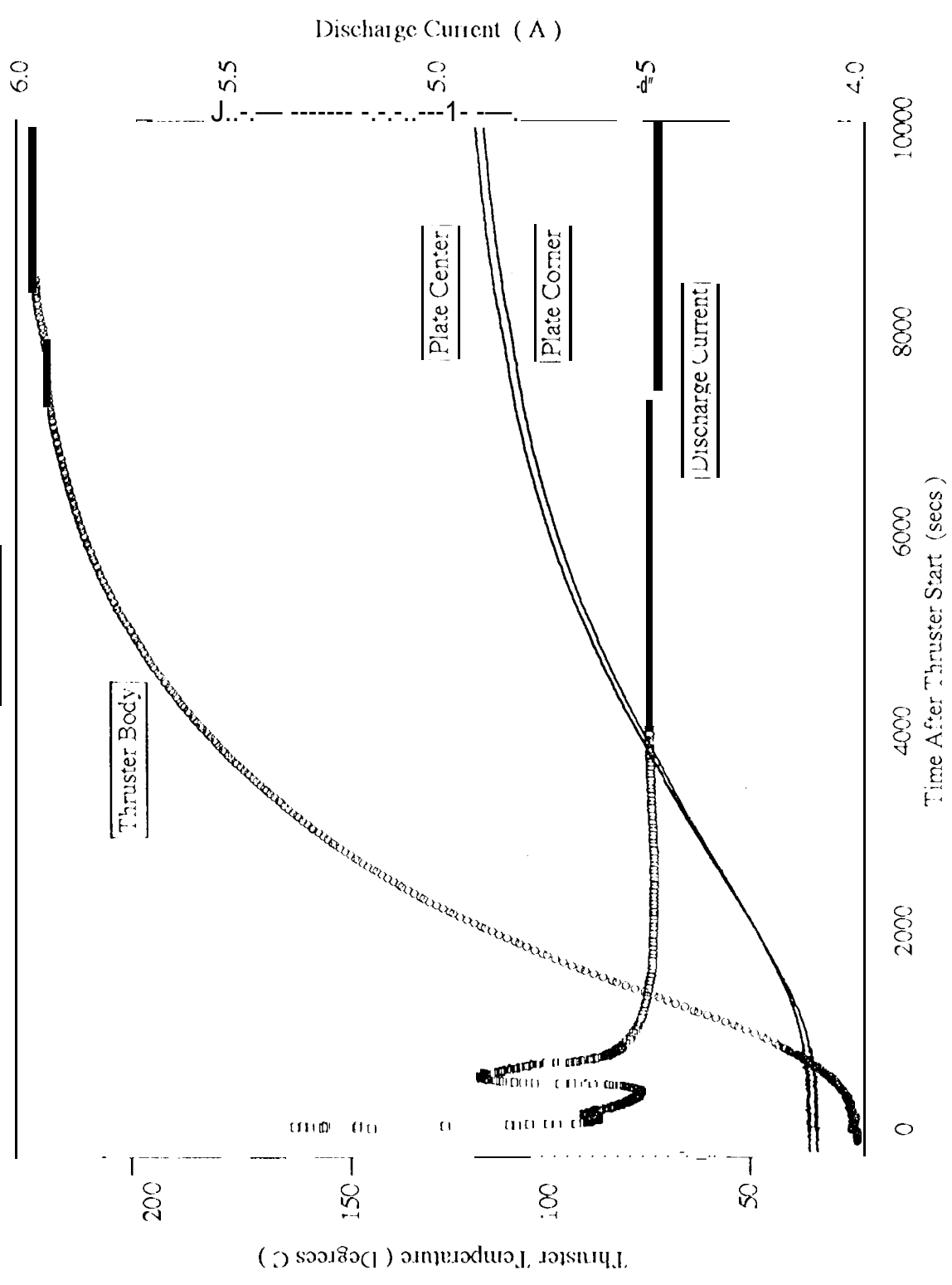


*Wear Test Results*

Fig. 4

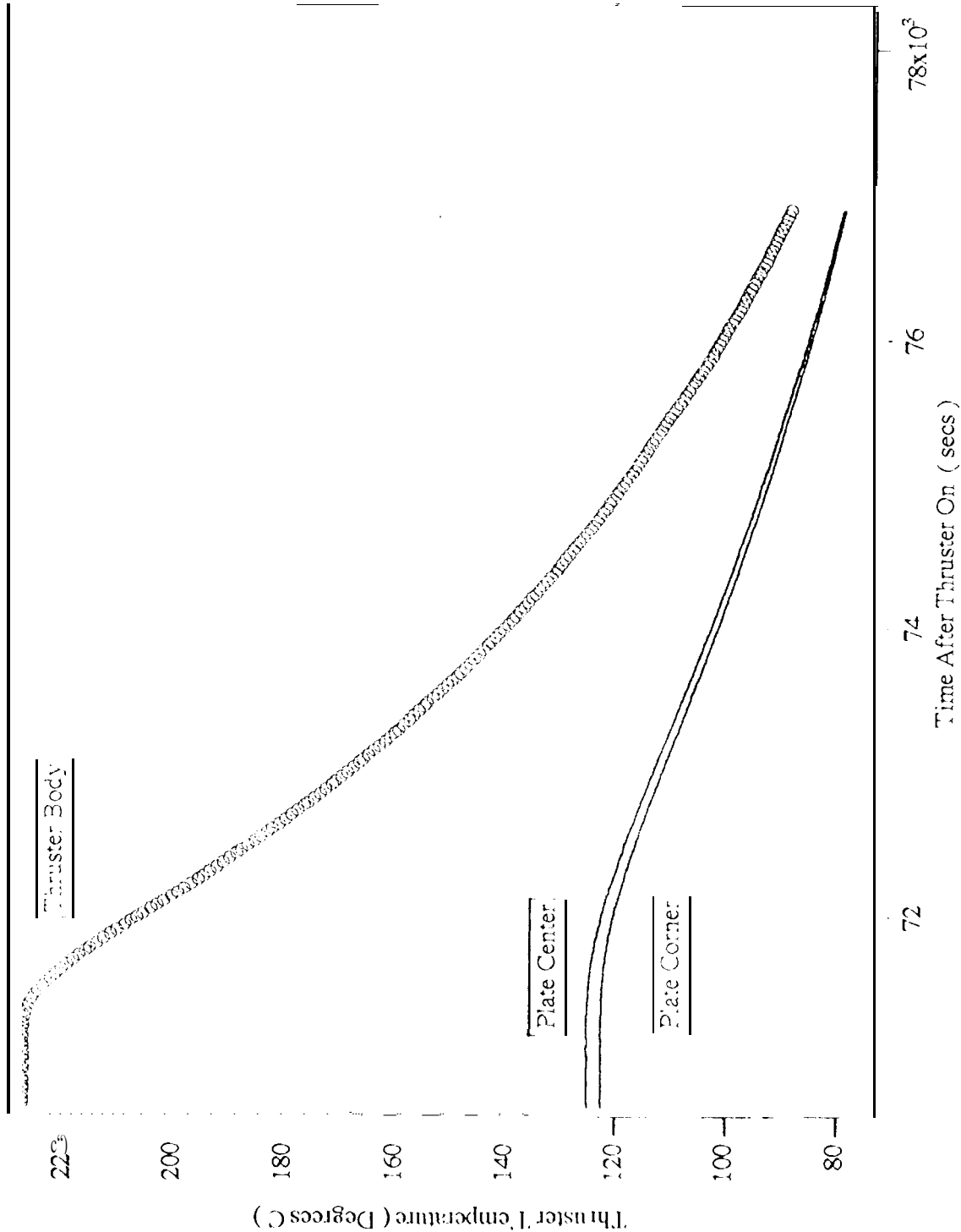
56

Cycle 56



Which Thruster?

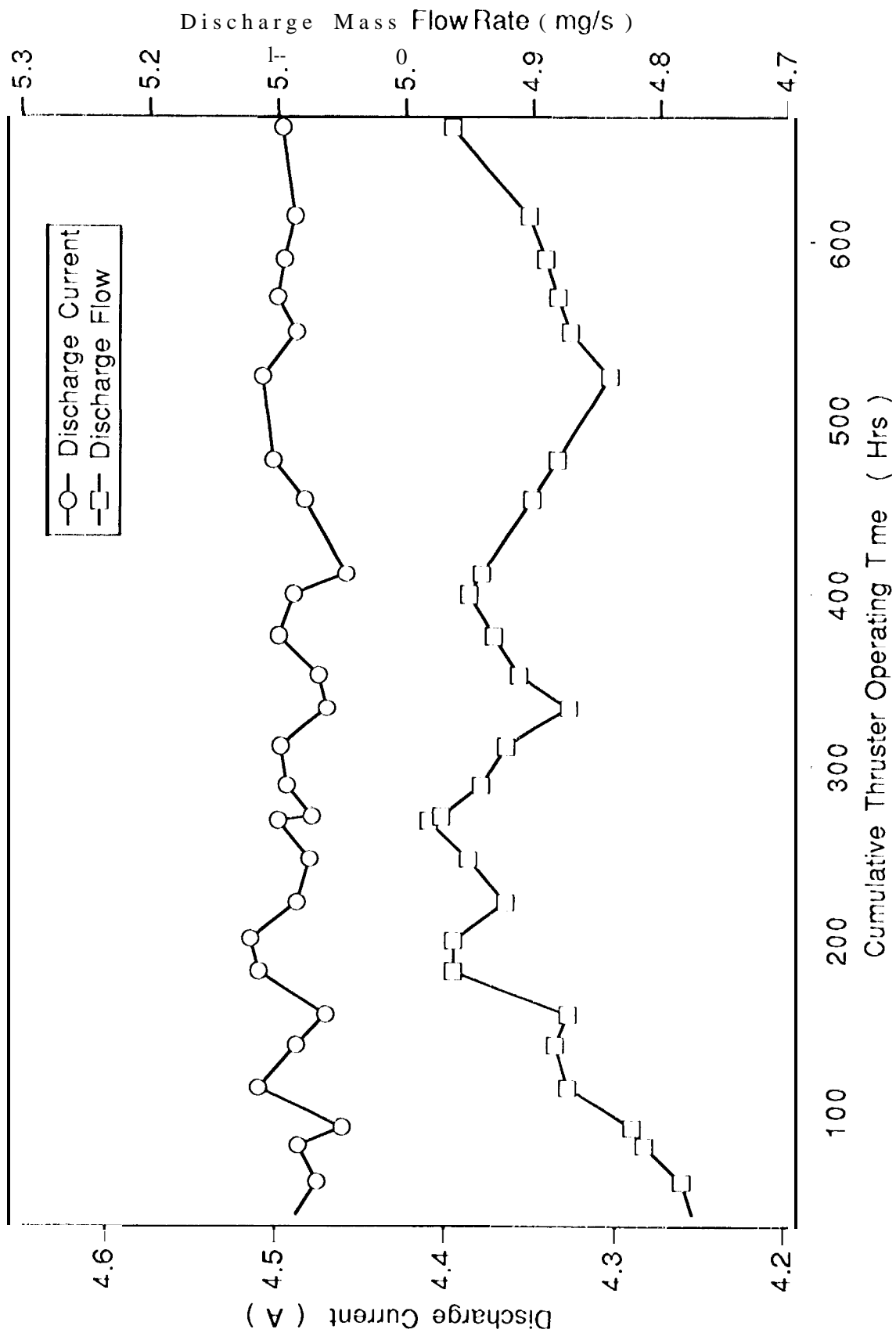
Cycle 56



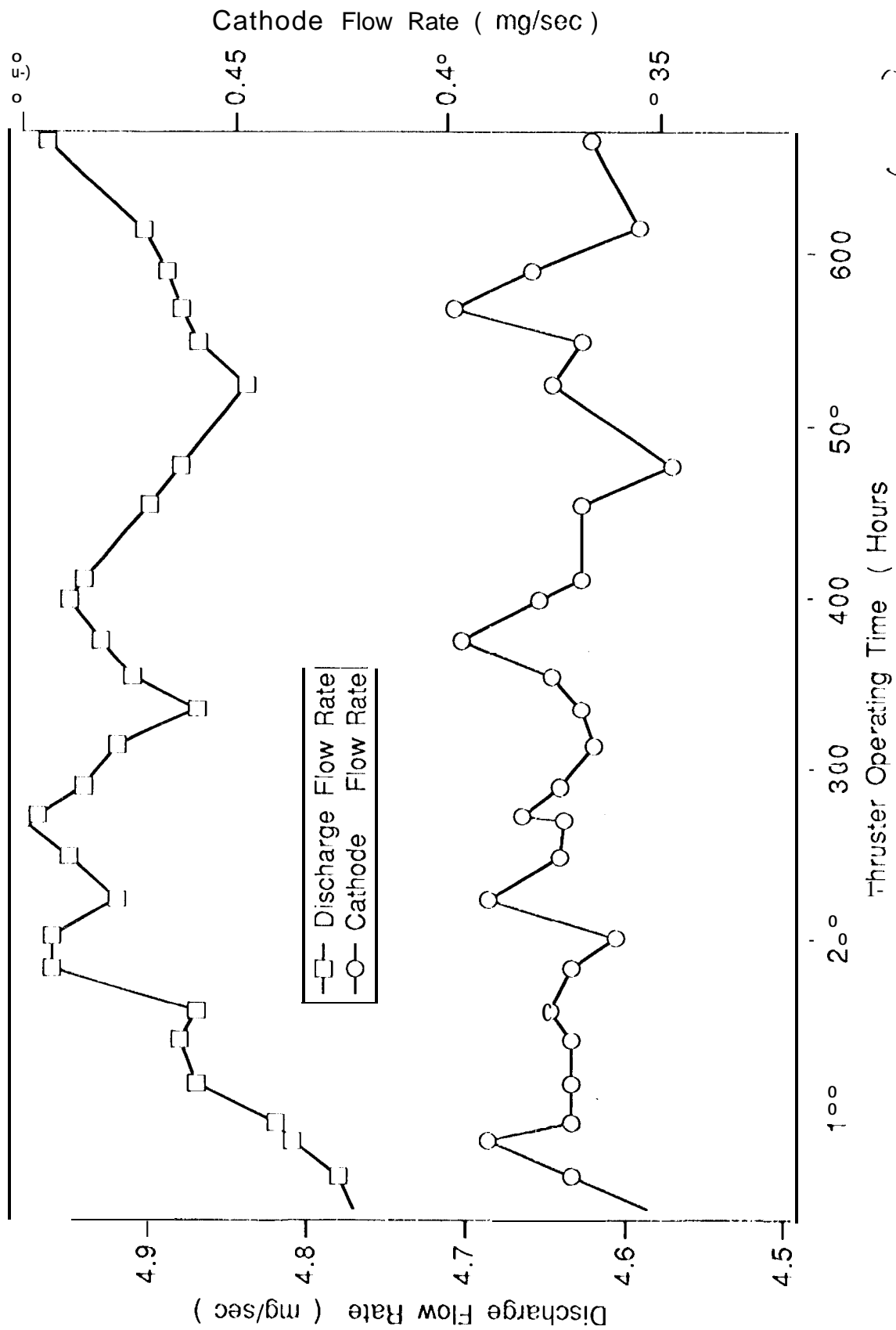
Where is  
"Push Off"  
Command?

Which Thruster?



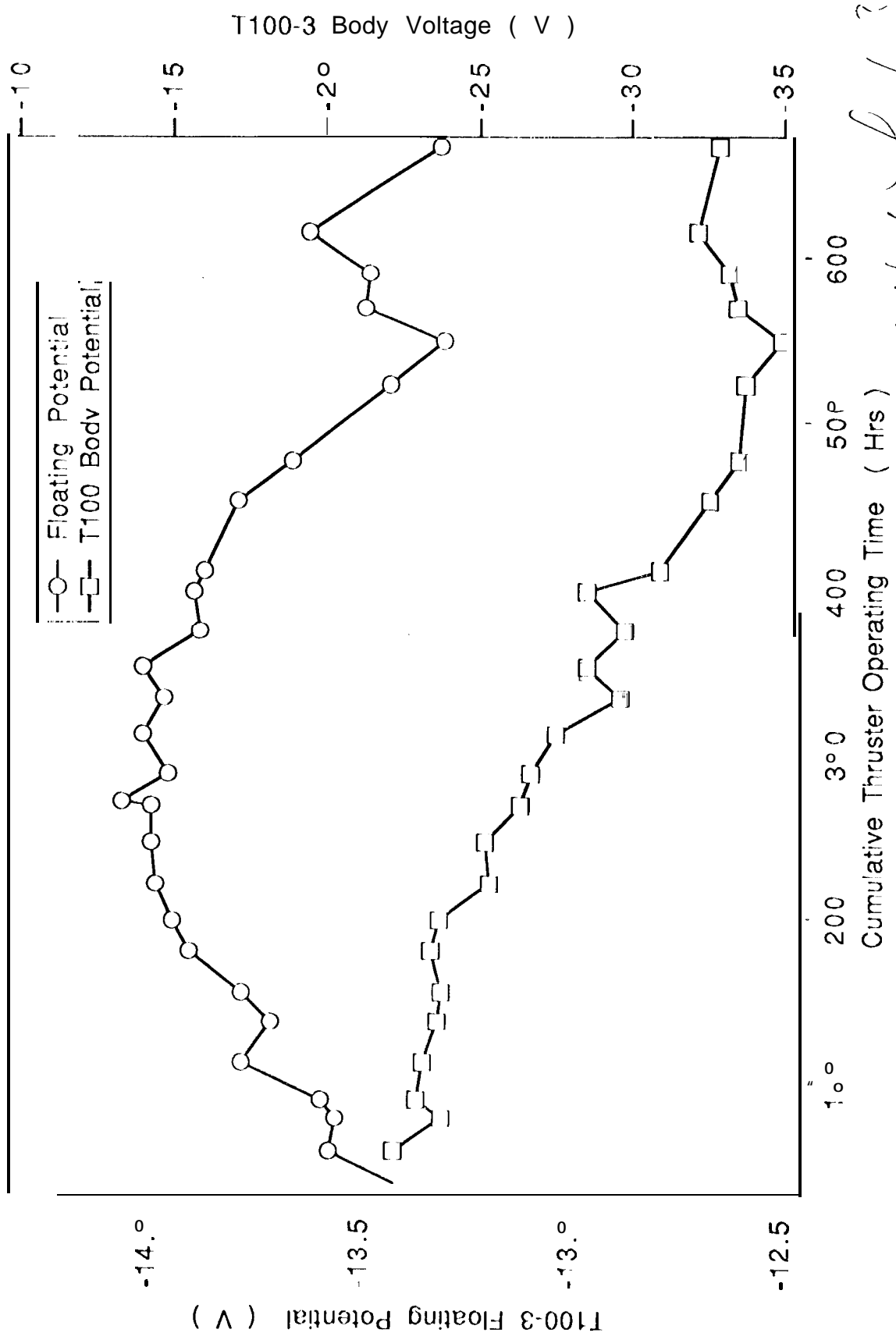


Which Thruster ?



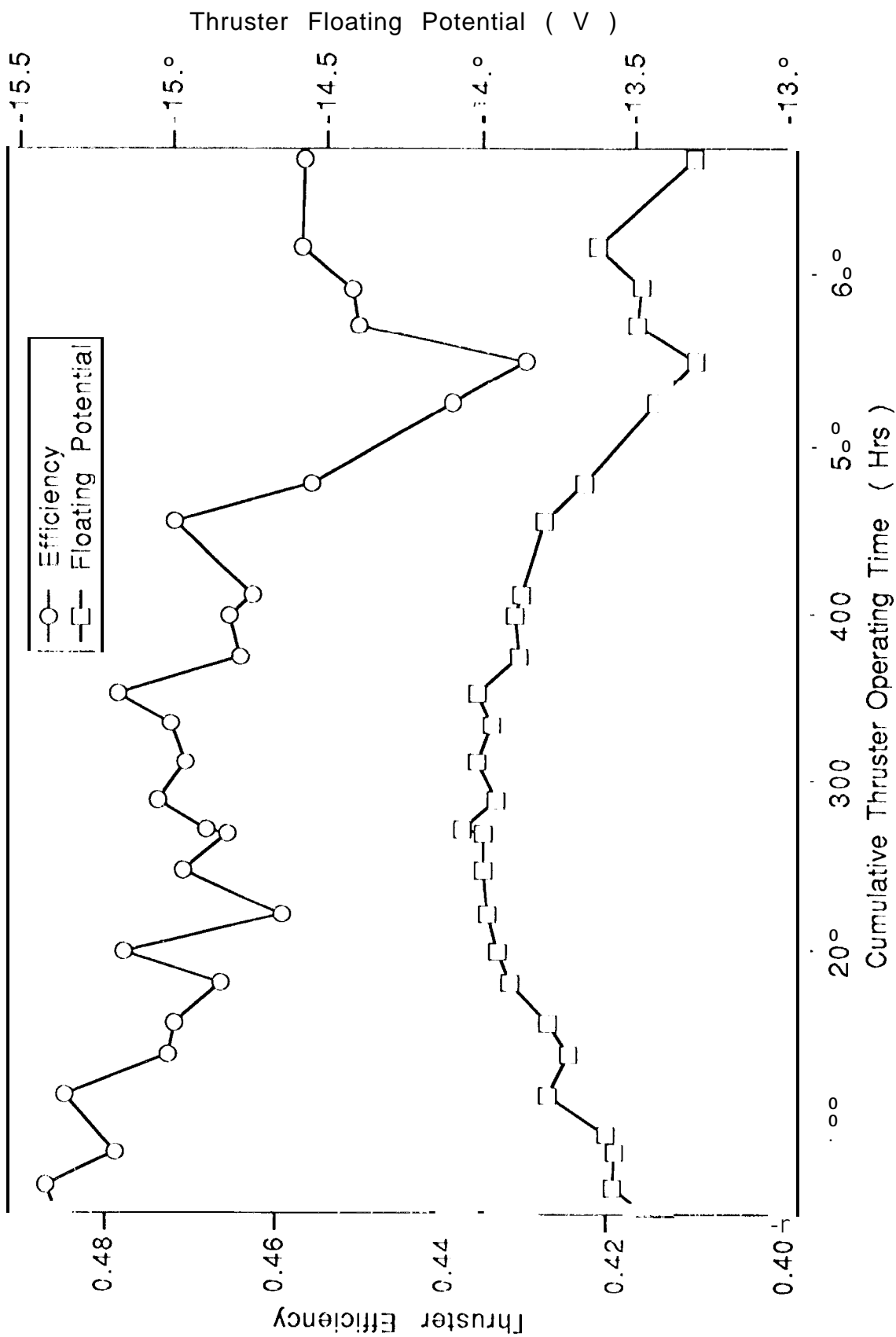
*Wick Thru?*

Fig 8



*Which Thruster ?*

690



*Which Thruster?*



Fig 11

Which Thruster

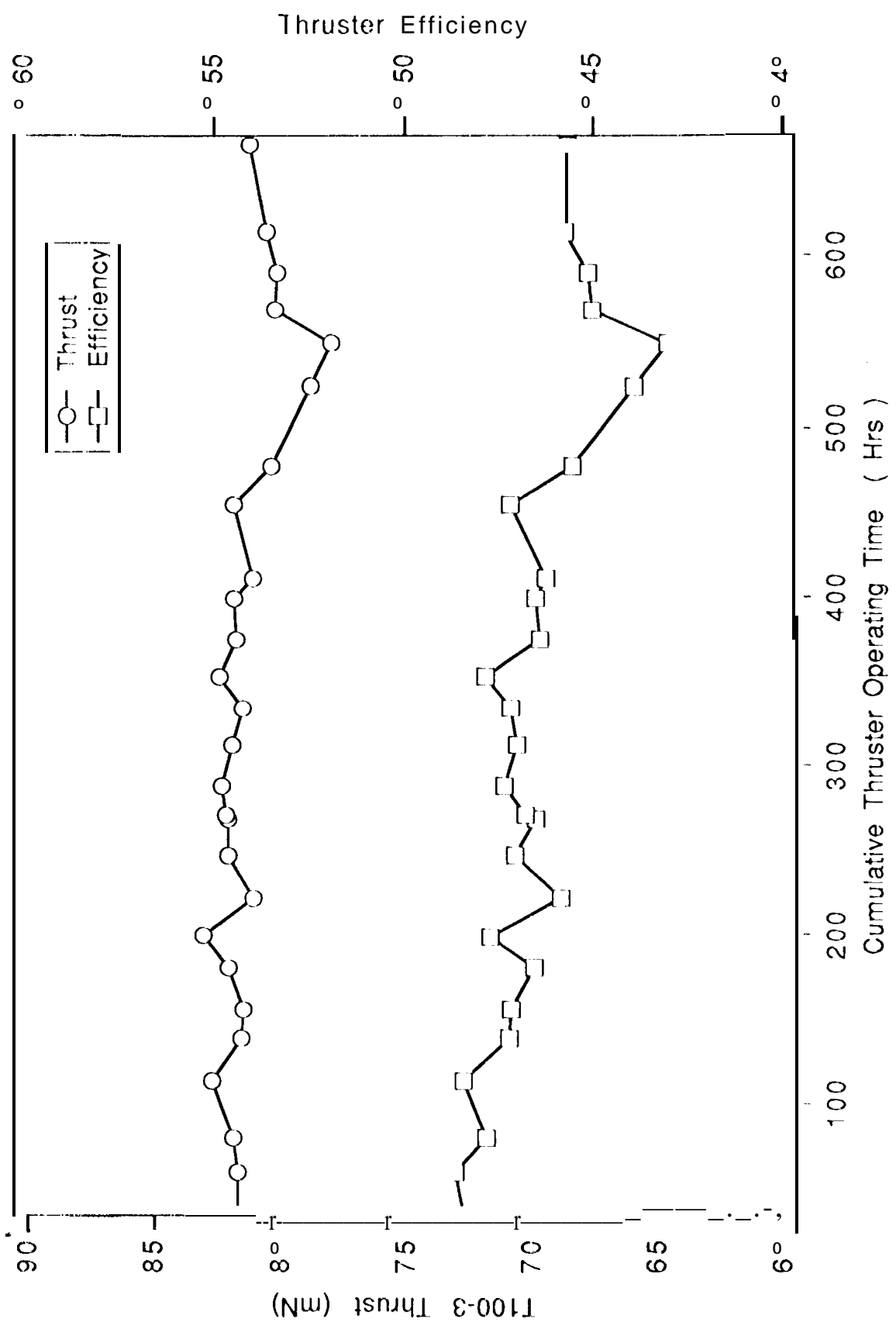
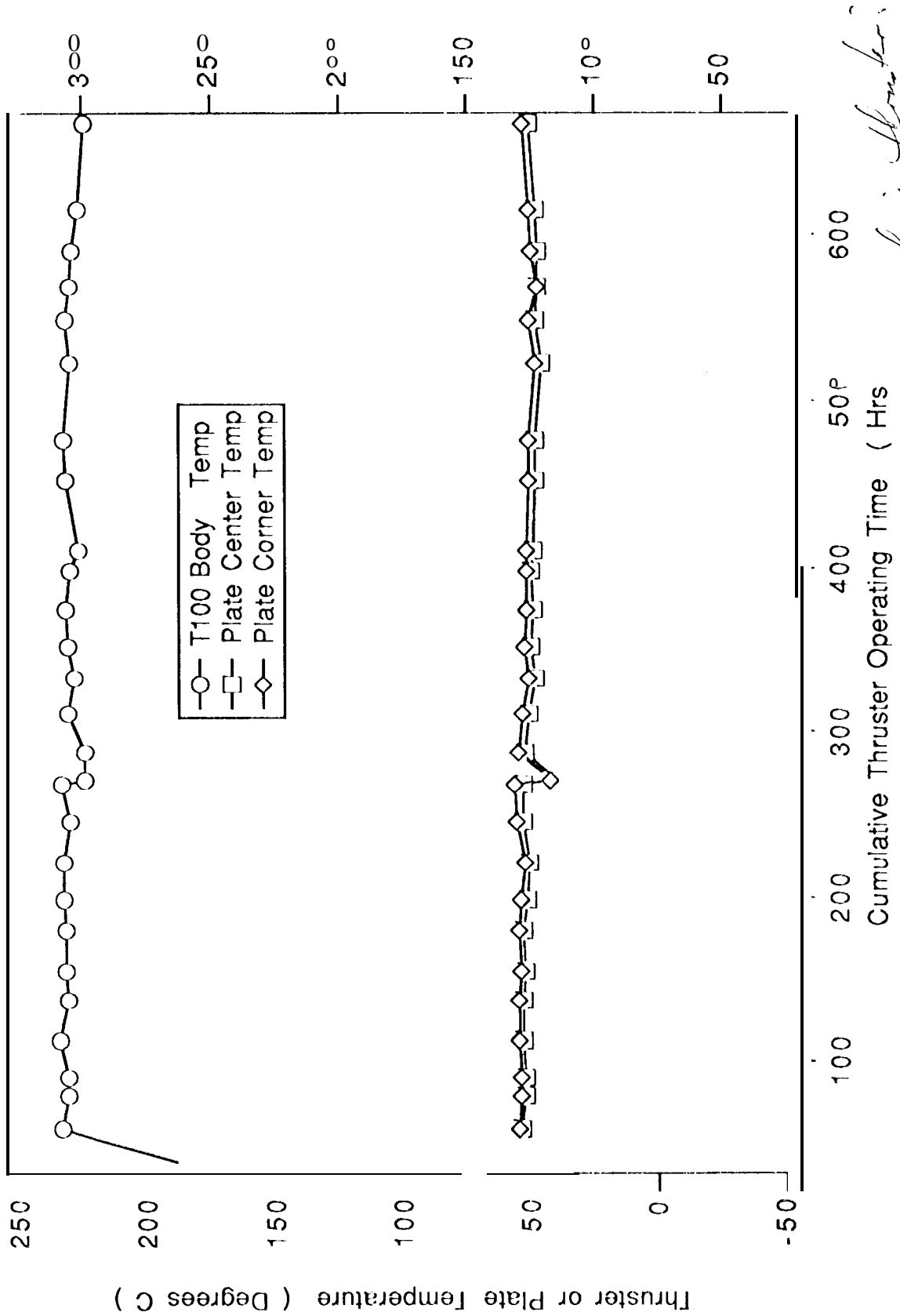


Fig 12 *Wich Thruster*

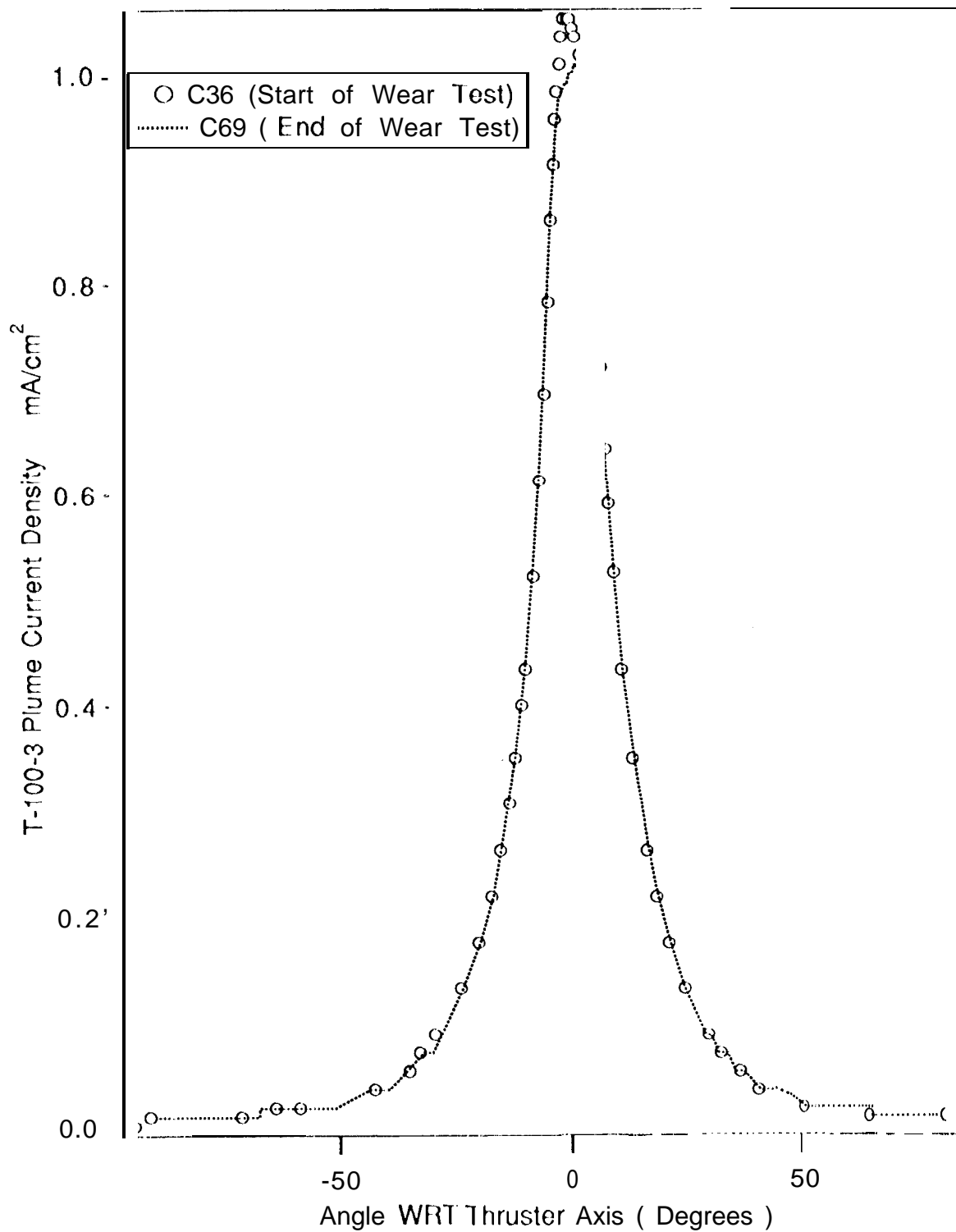


*which fluctuates*

*which fluctuates*

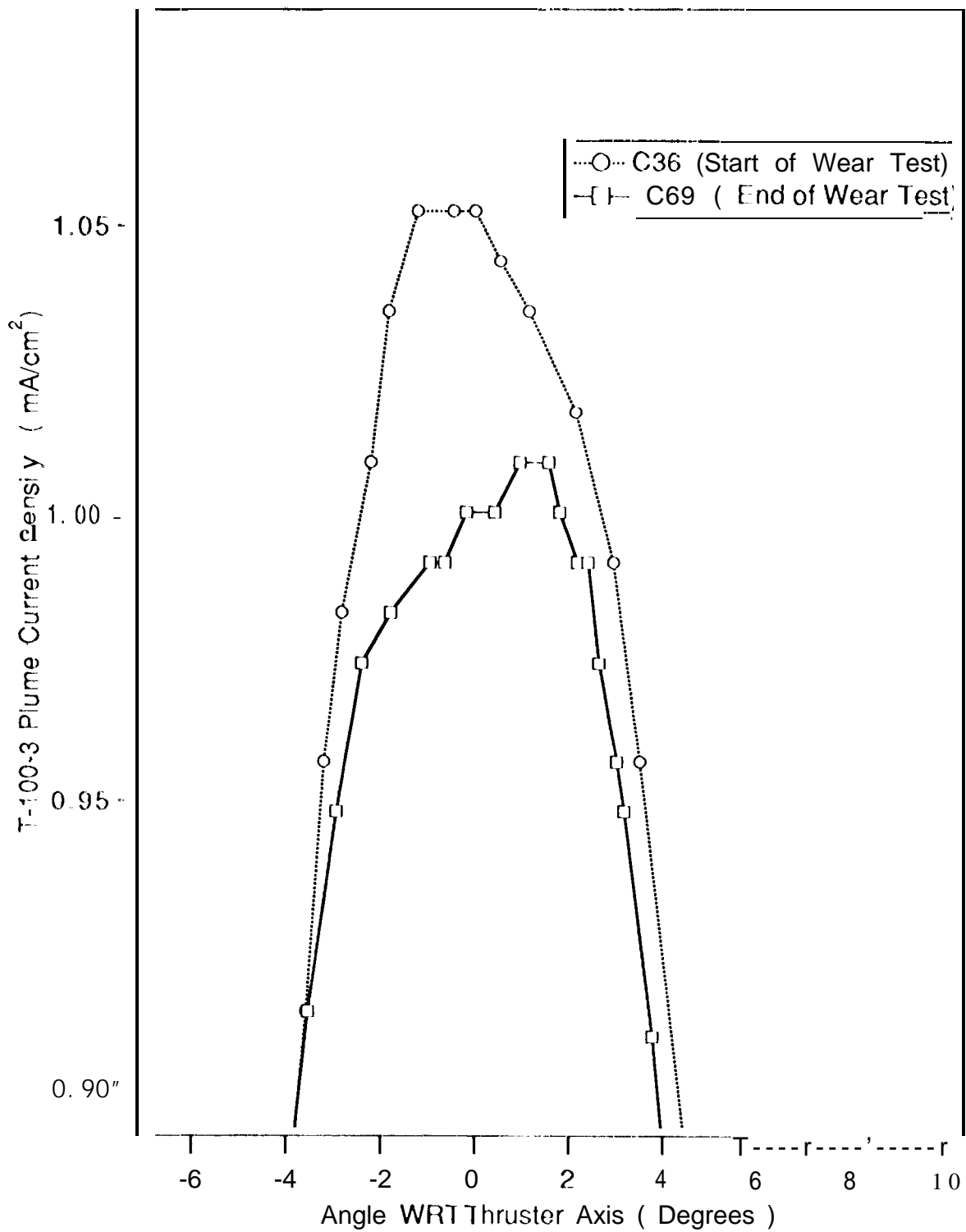
Fig 3





*Wish House*

Fig 14



with thruster

fig 15

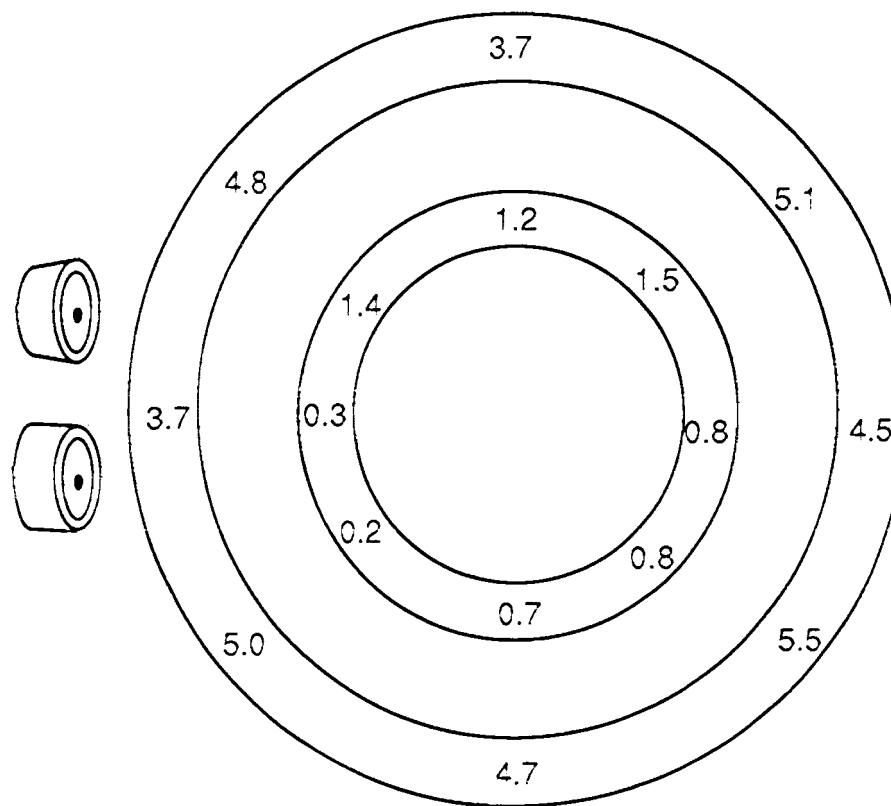


Fig. 16. Insulator erosion in the T-100-3" after completion of the 632-hr wear test. Numbers denote erosion of the insulator in millimeters.

*which thrust?*

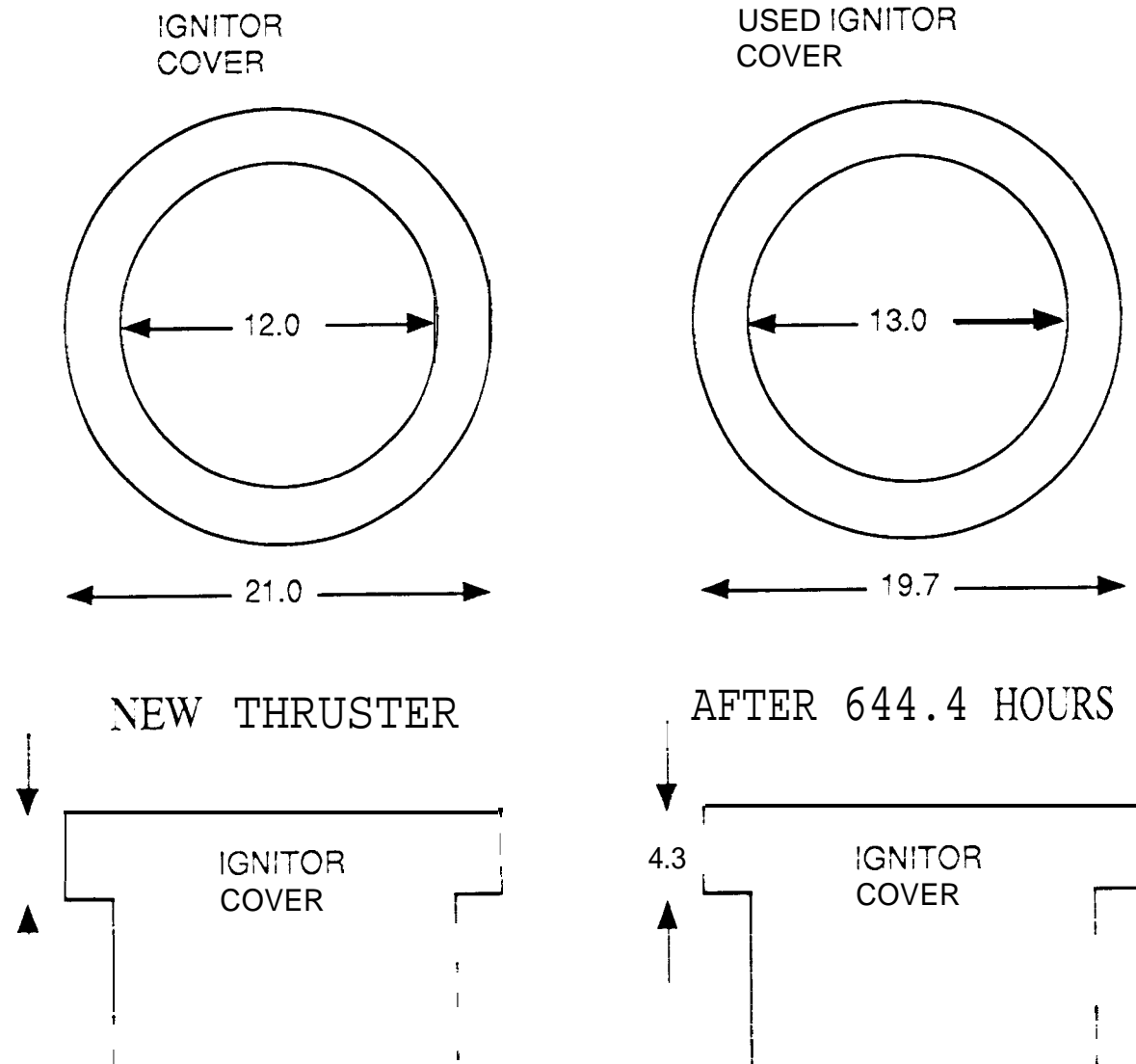
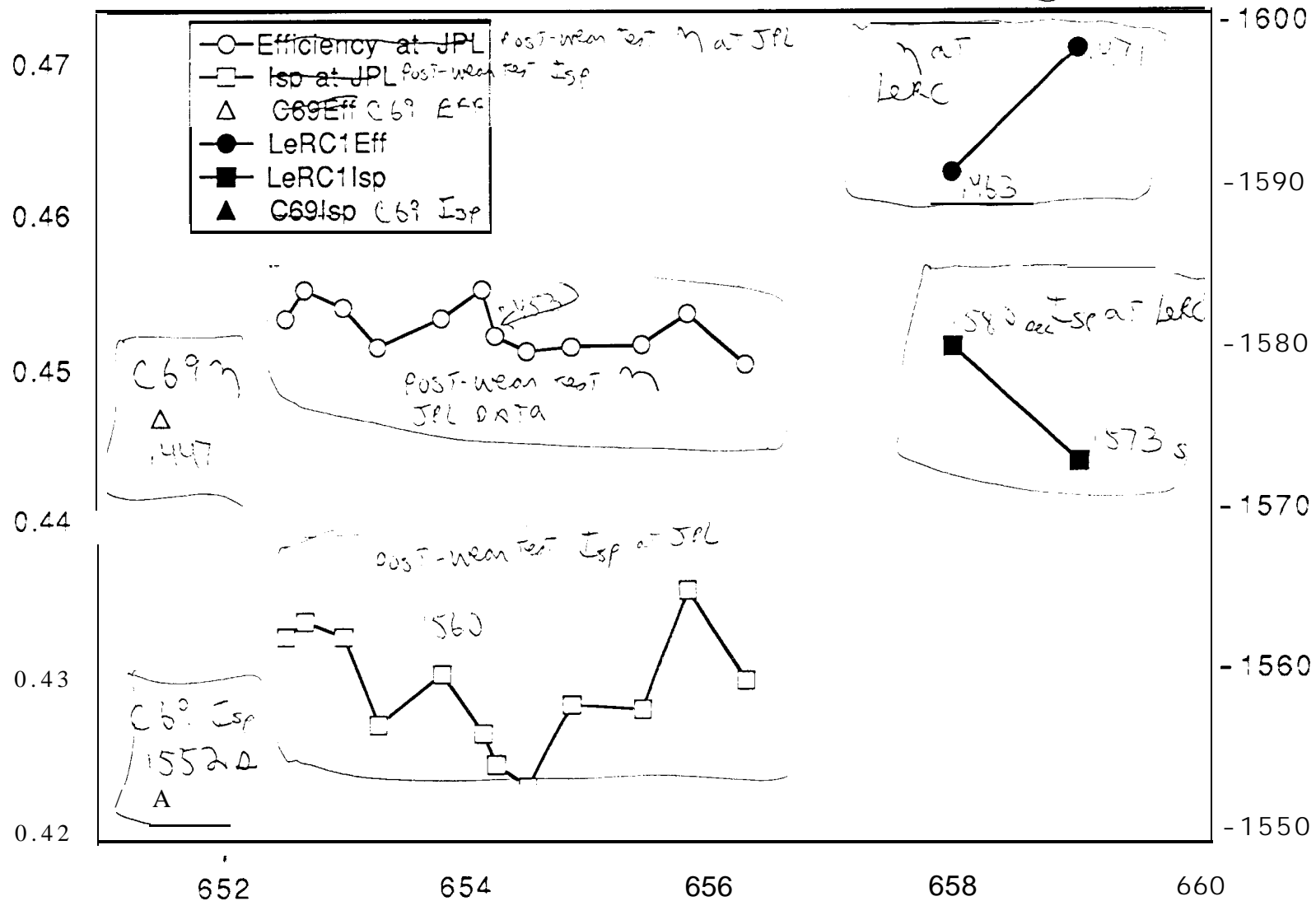


Fig. 17. Ignitor cover wear before and at the completion of the wear test. Numbers denote erosion in mm.

*which thruster?*

Fig 10



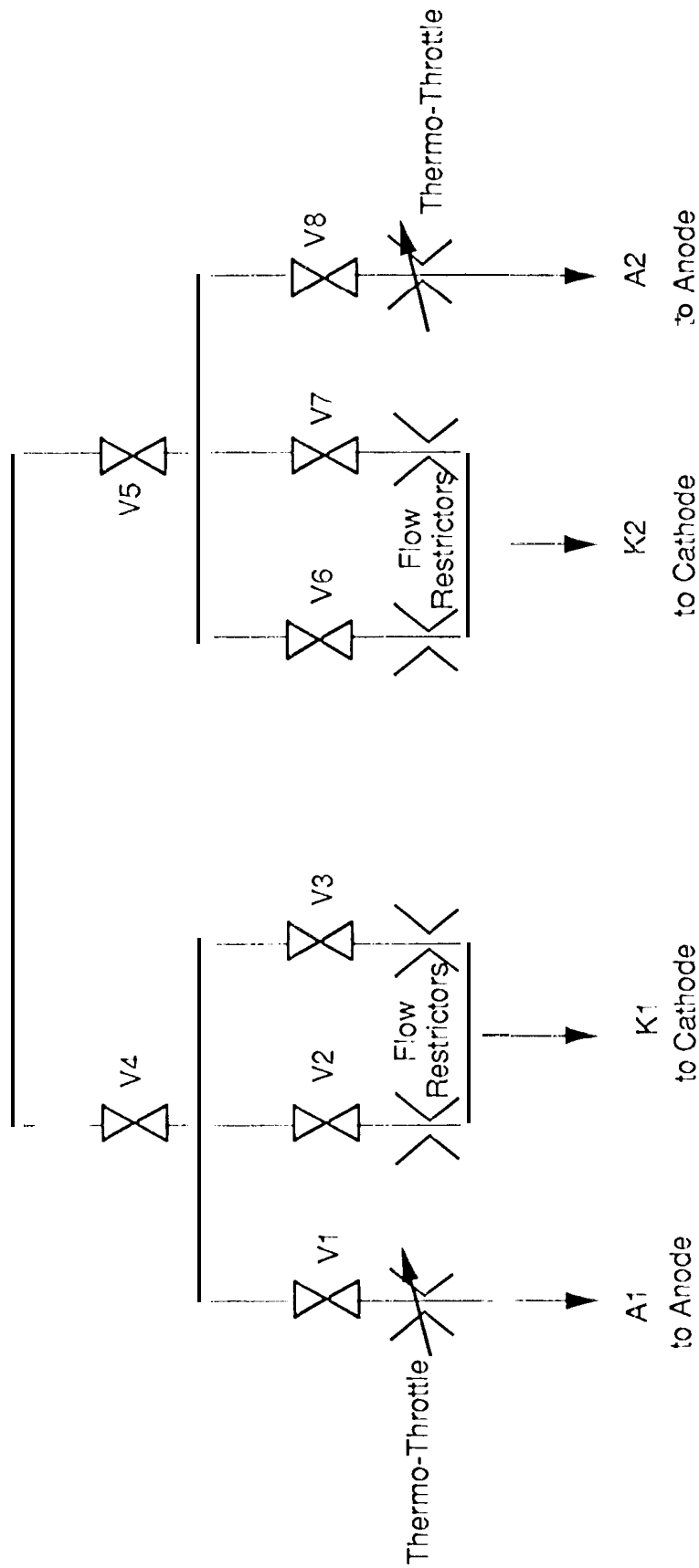
which thruster?

10

Fig

1

Inlet



1

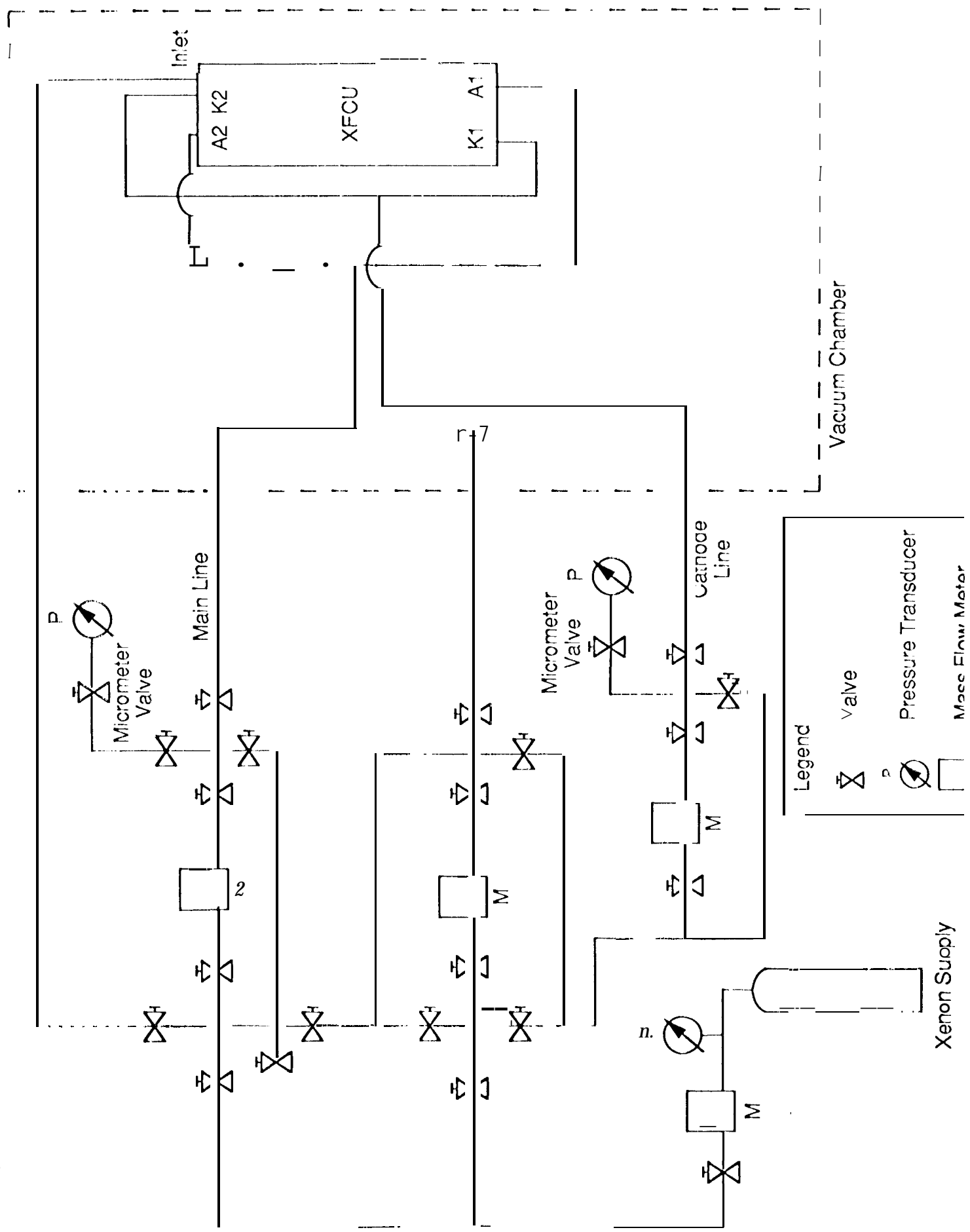




Fig. 21

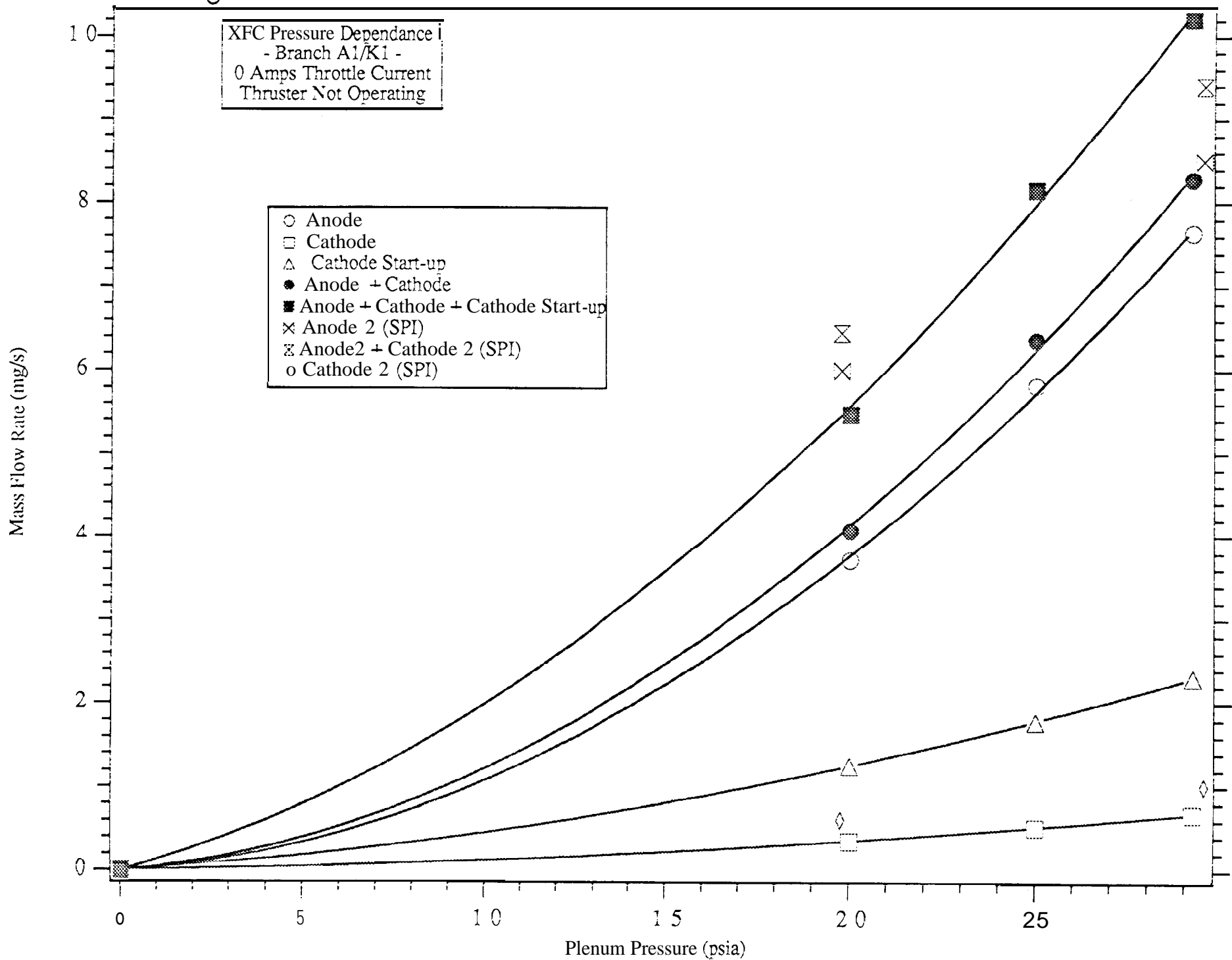
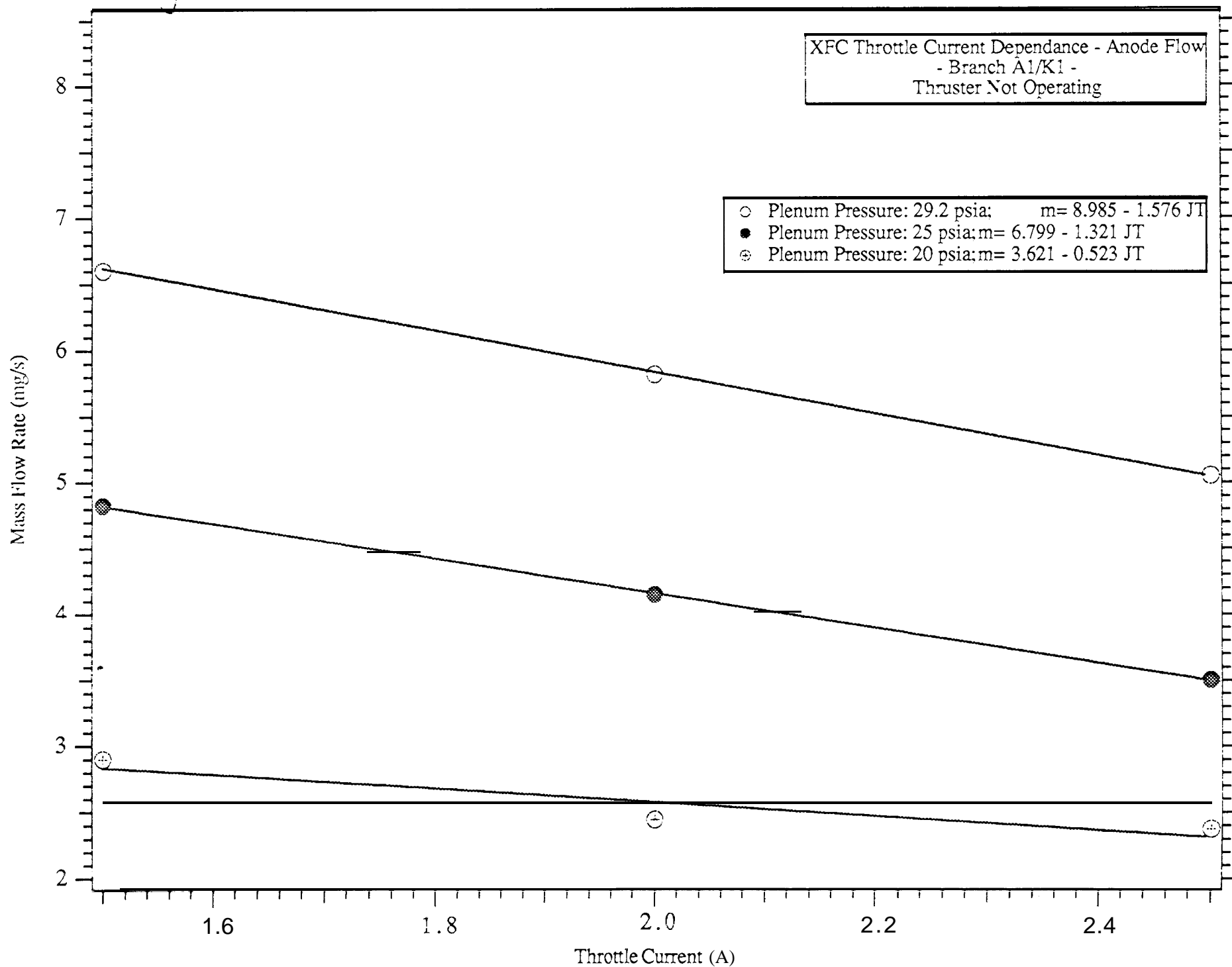


Fig 22



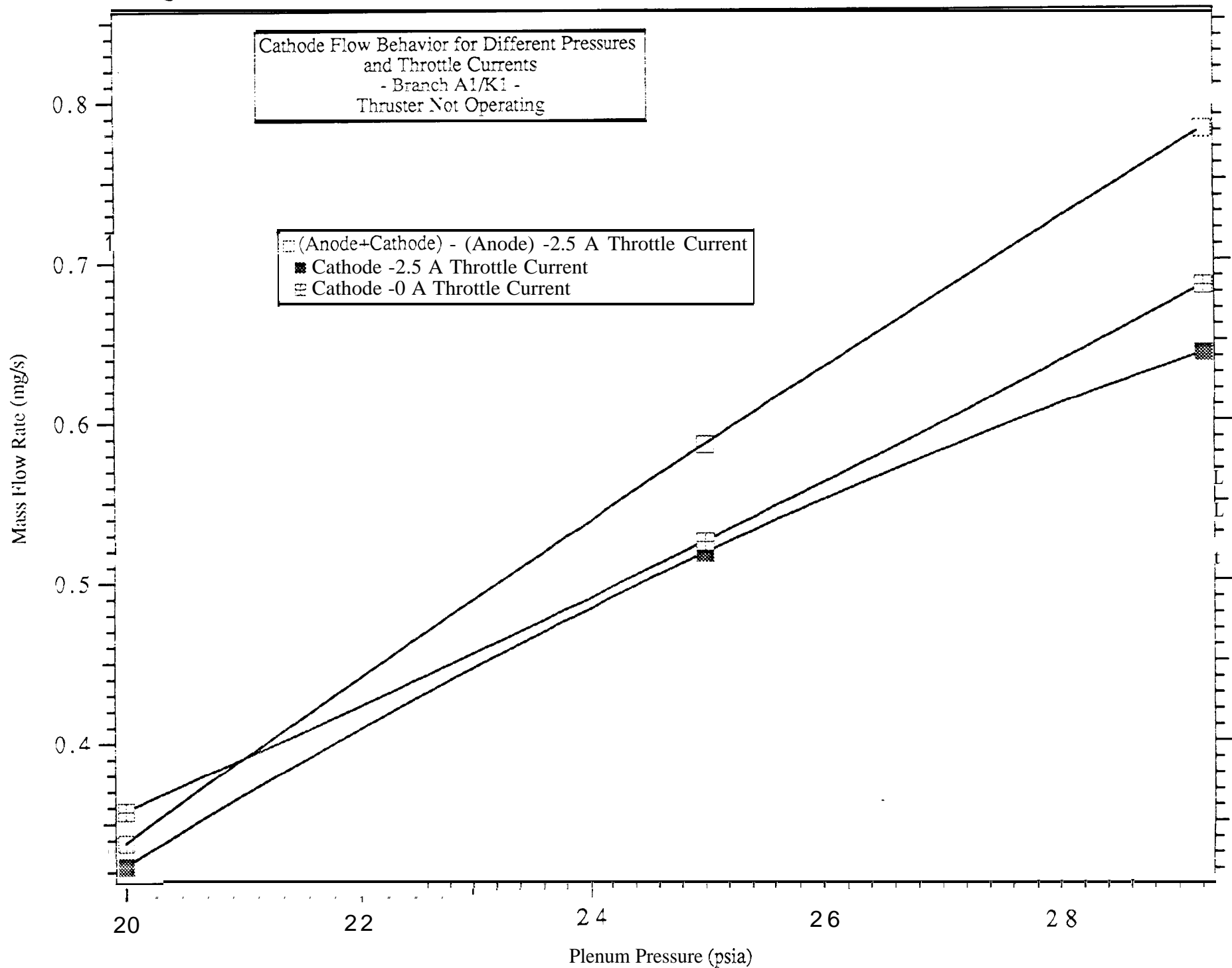


Fig 26

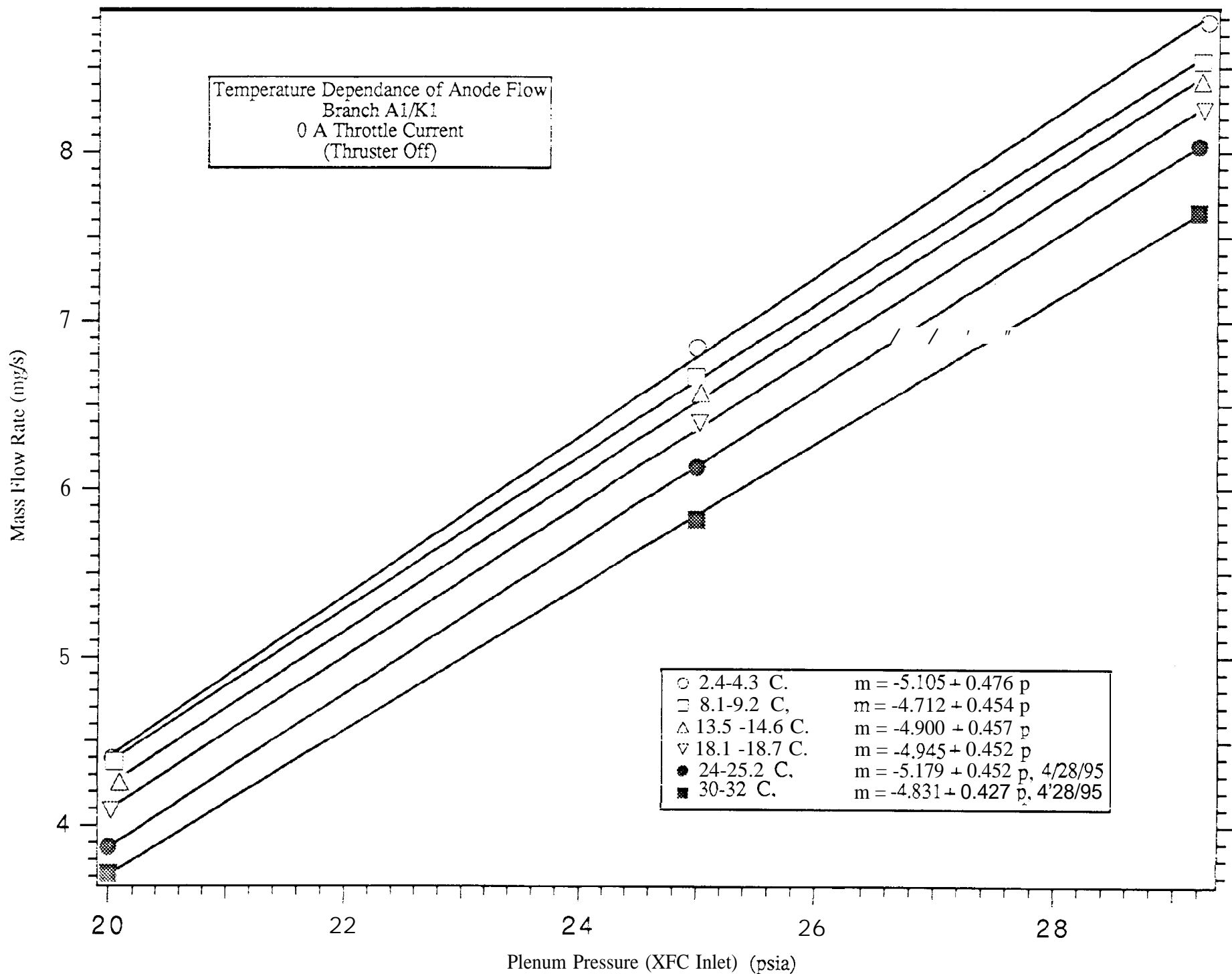


Fig 2/5

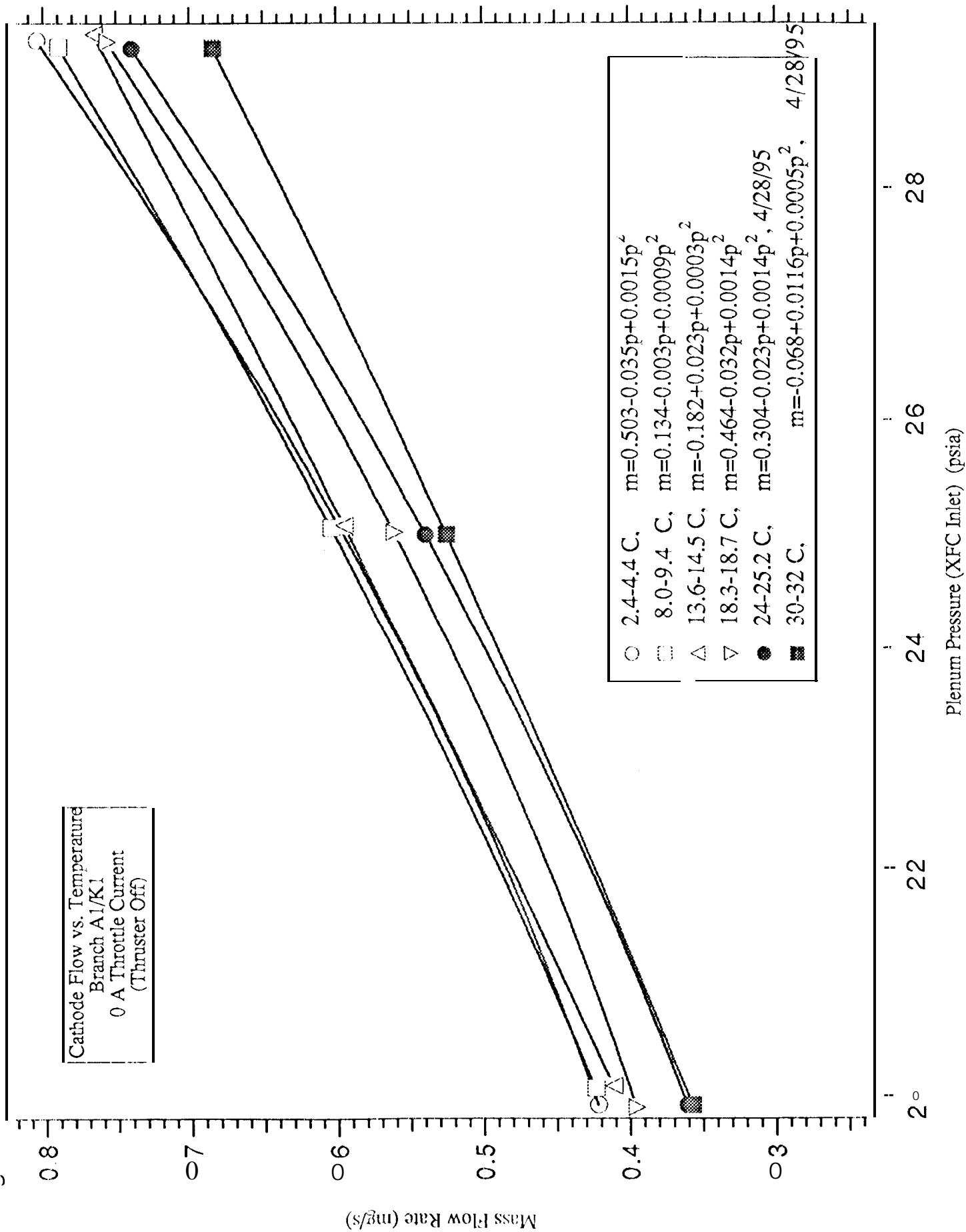


Fig 26

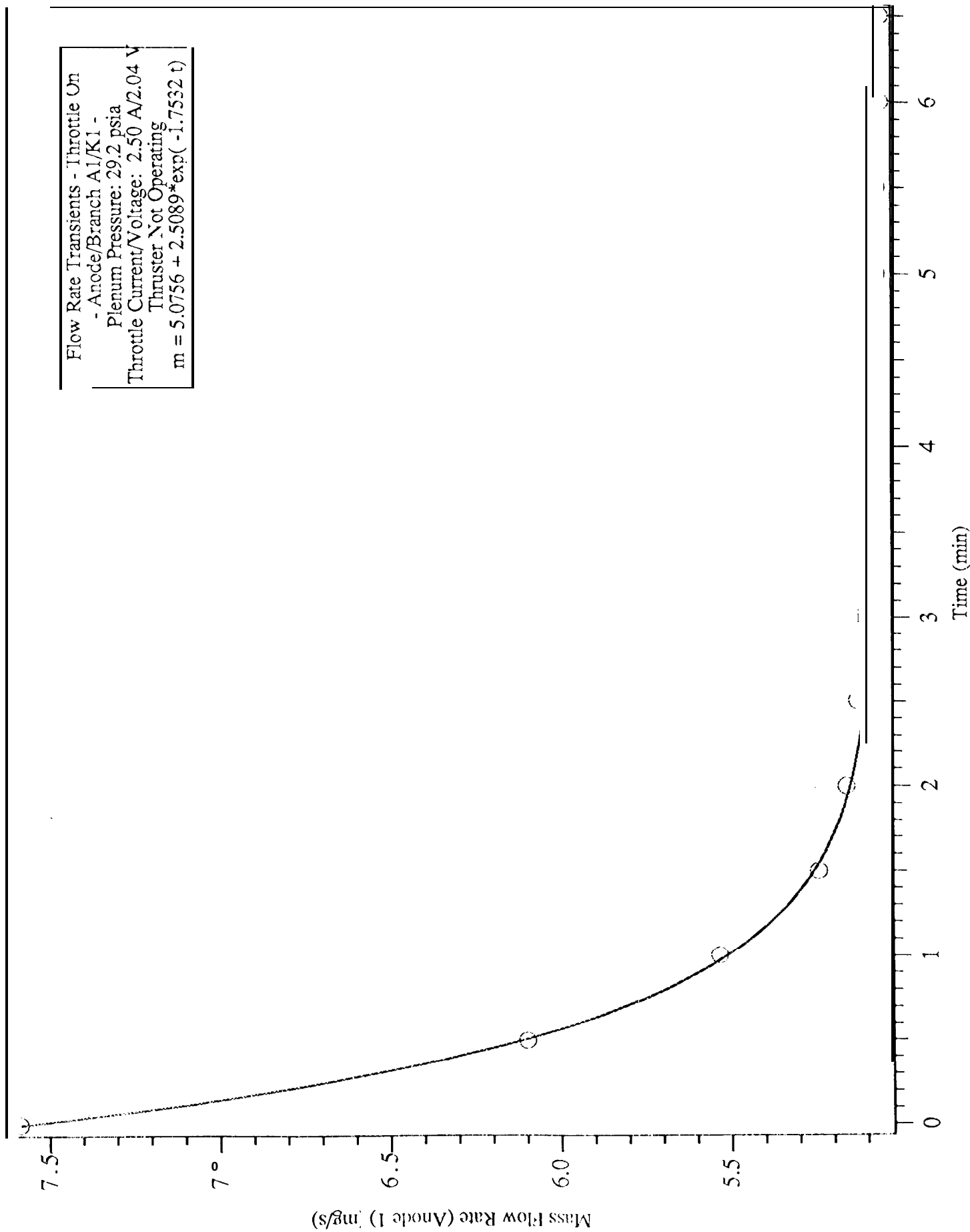
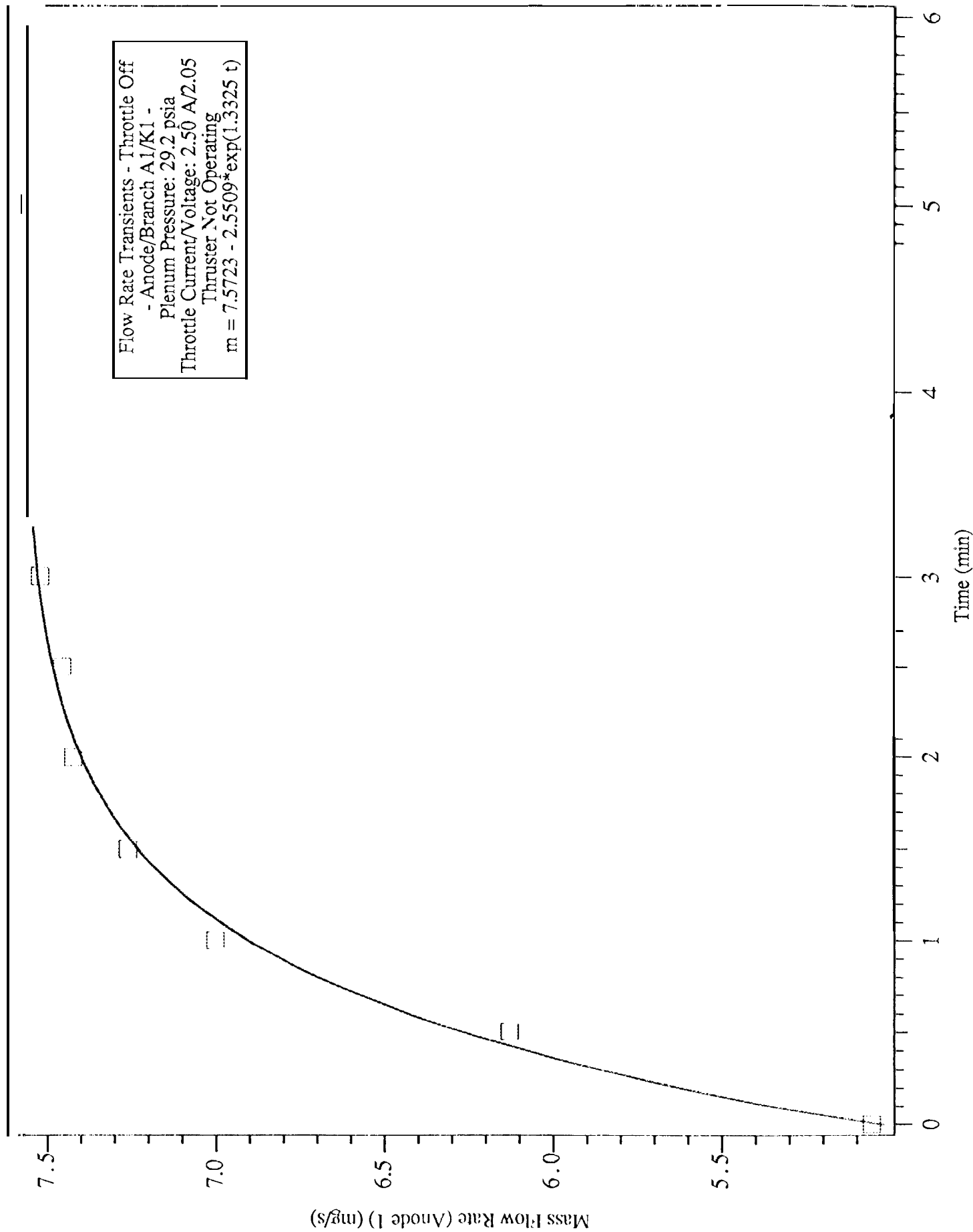
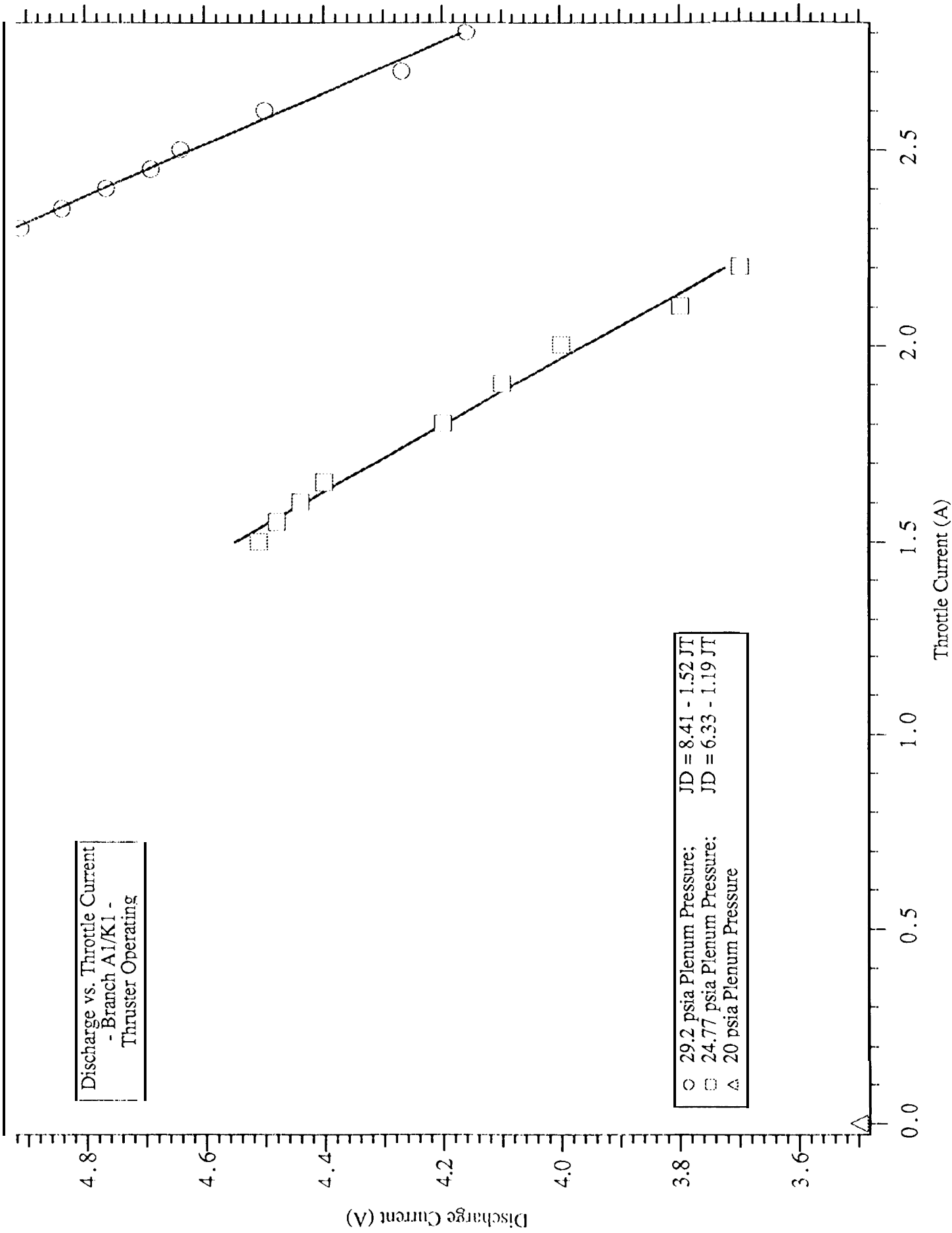


Fig 27



Discharge vs. Throttle Current  
- Branch A1/K1 -  
Thruster Operating

○ 29.2 psia Plenum Pressure; JD = 8.41 - 1.52 JT  
□ 24.77 psia Plenum Pressure; JD = 6.33 - 1.19 JT  
△ 20 psia Plenum Pressure





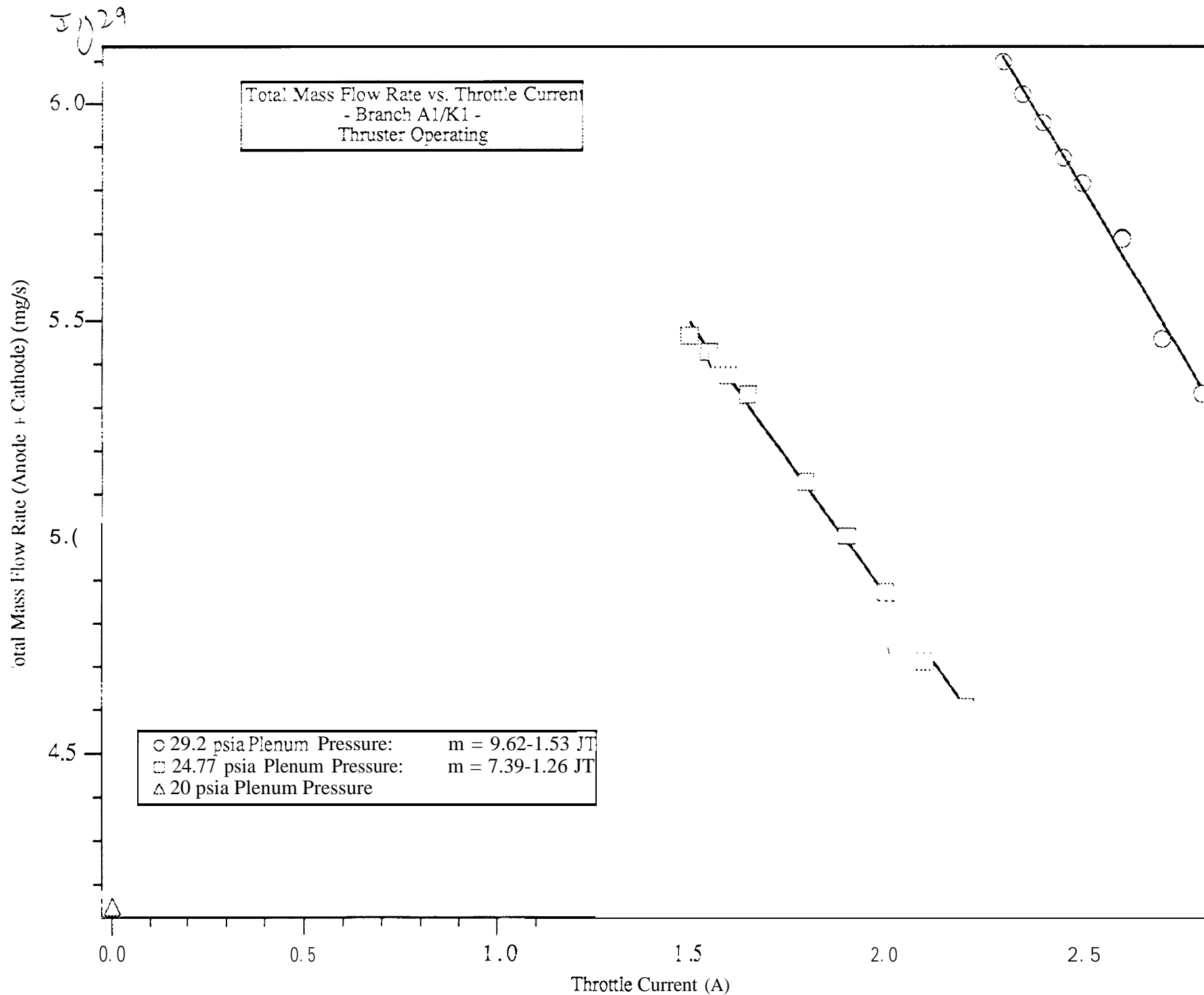


Fig 30.

Discharge Current vs. Throttle Power  
- Branch A1/K1 -  
Thruster Operating

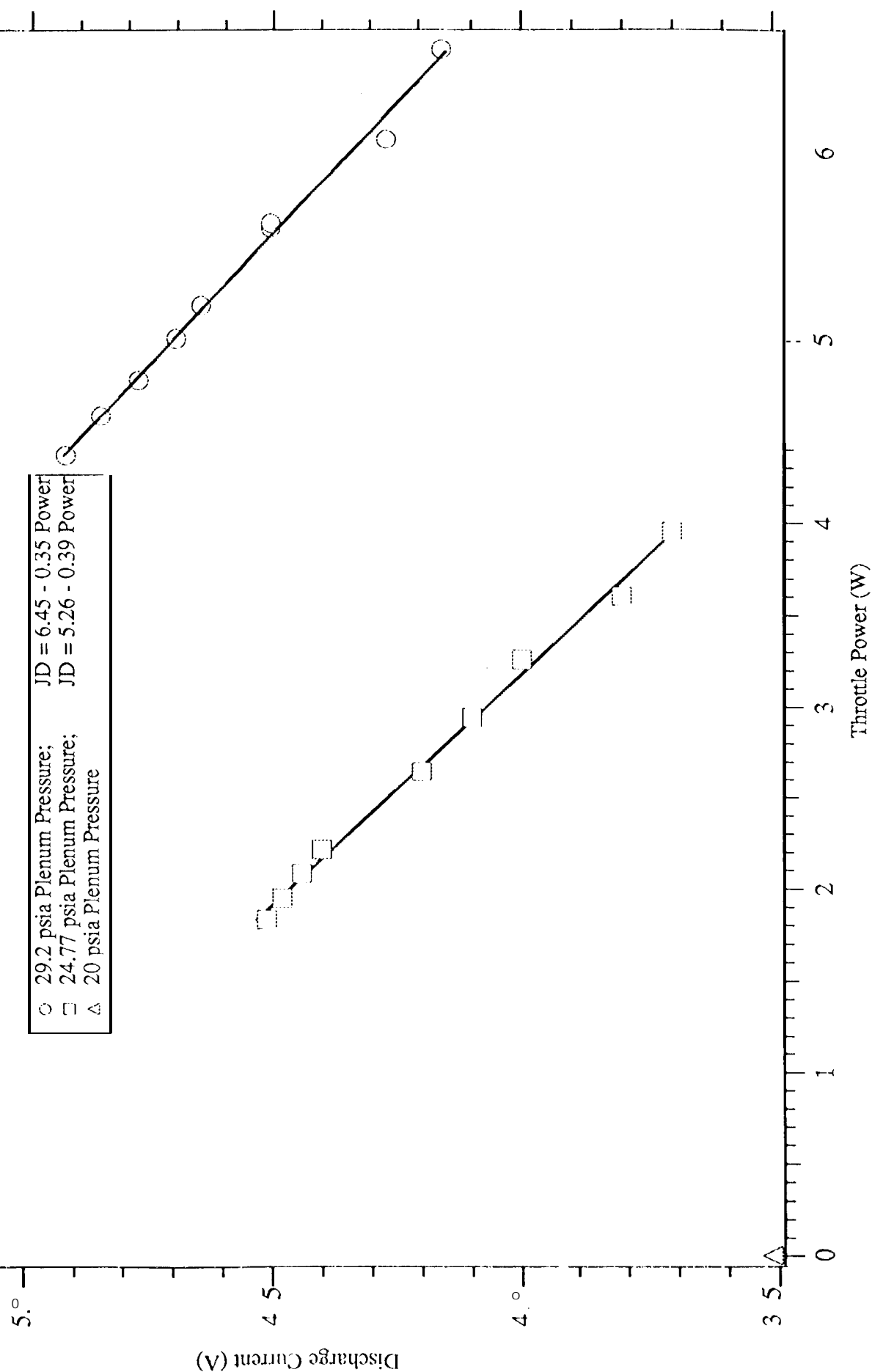
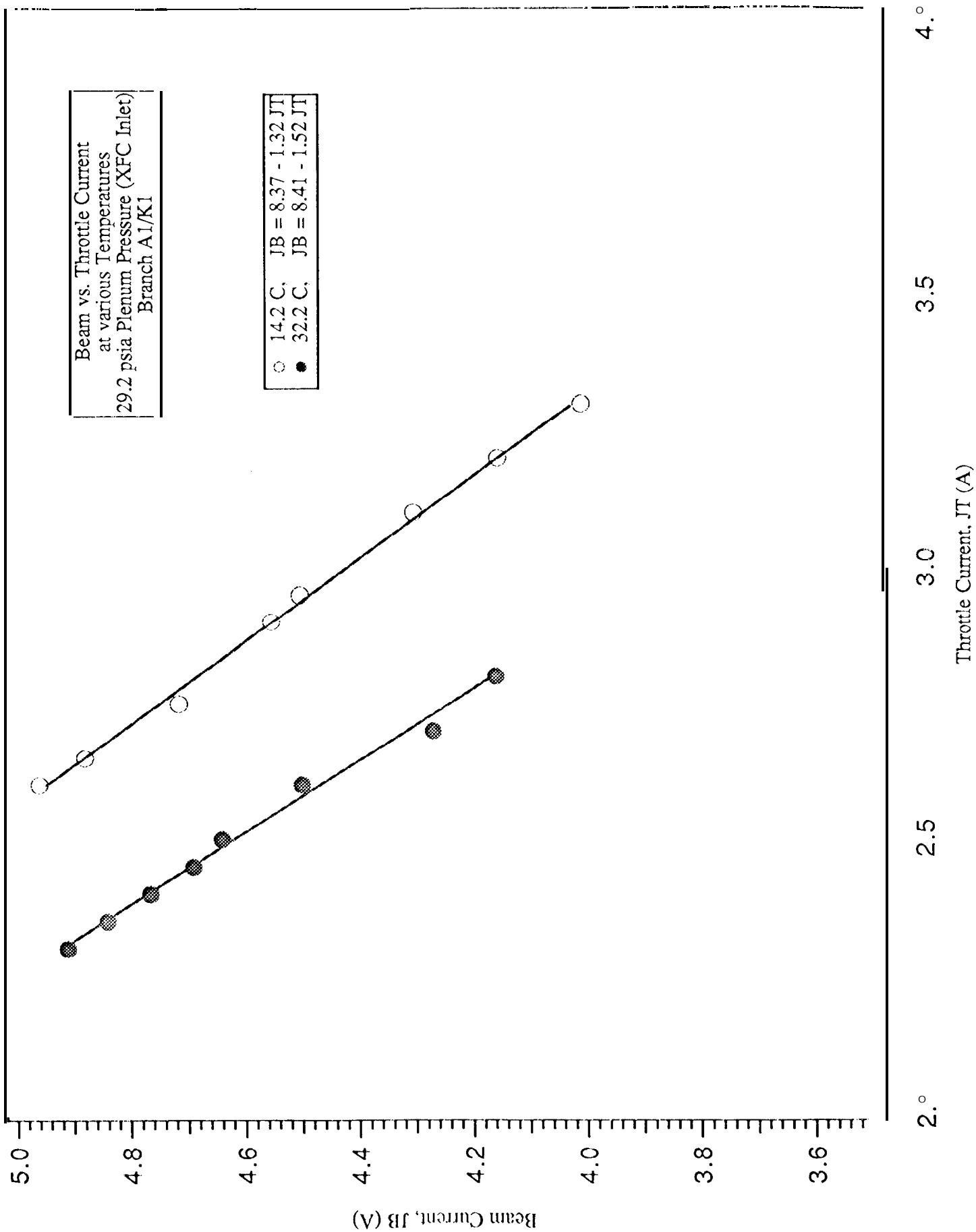
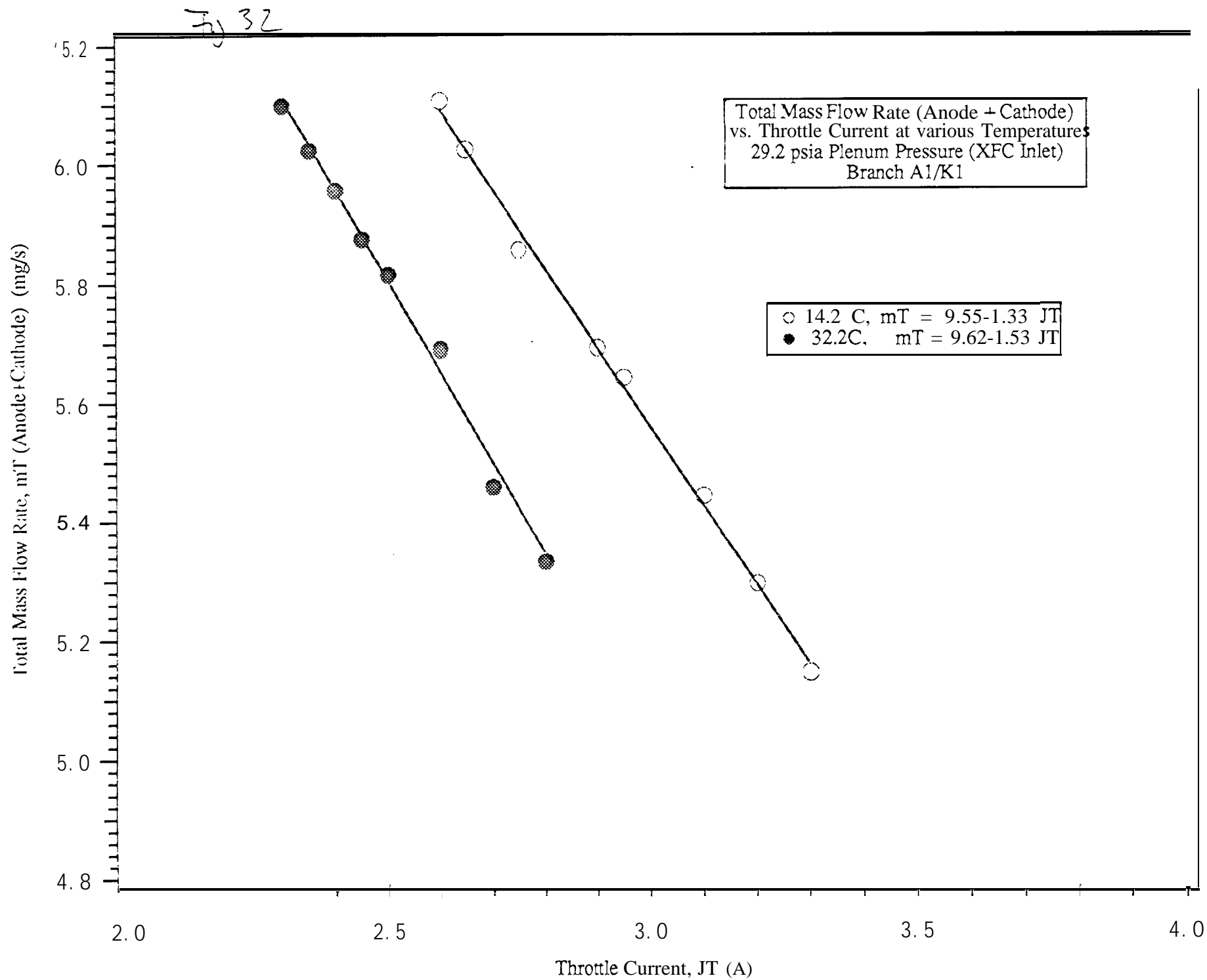
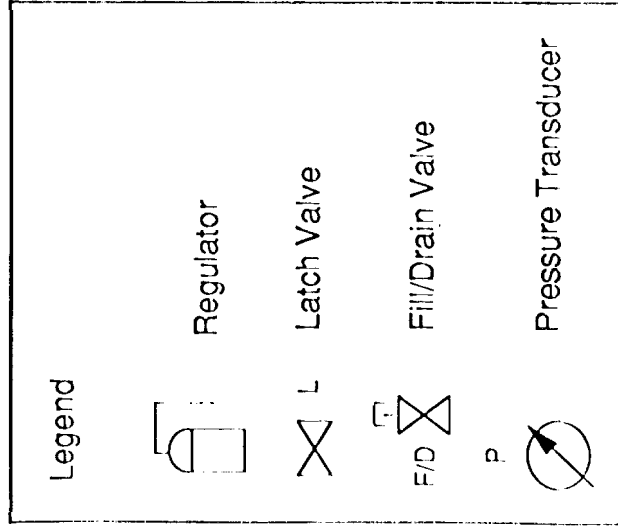
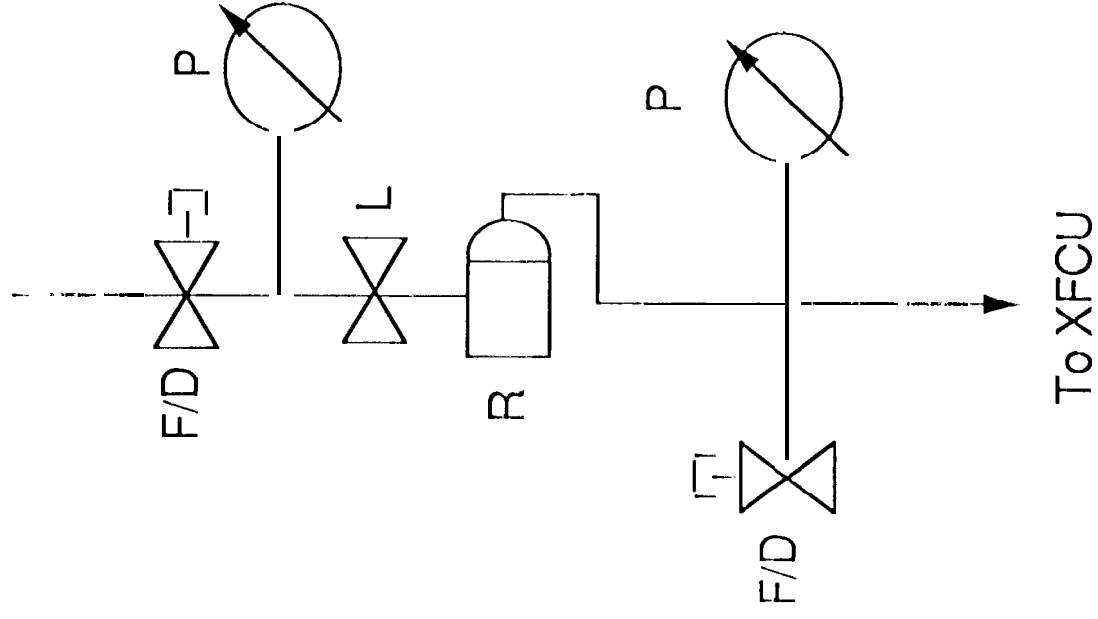


Fig. 31





From Xenon Supply



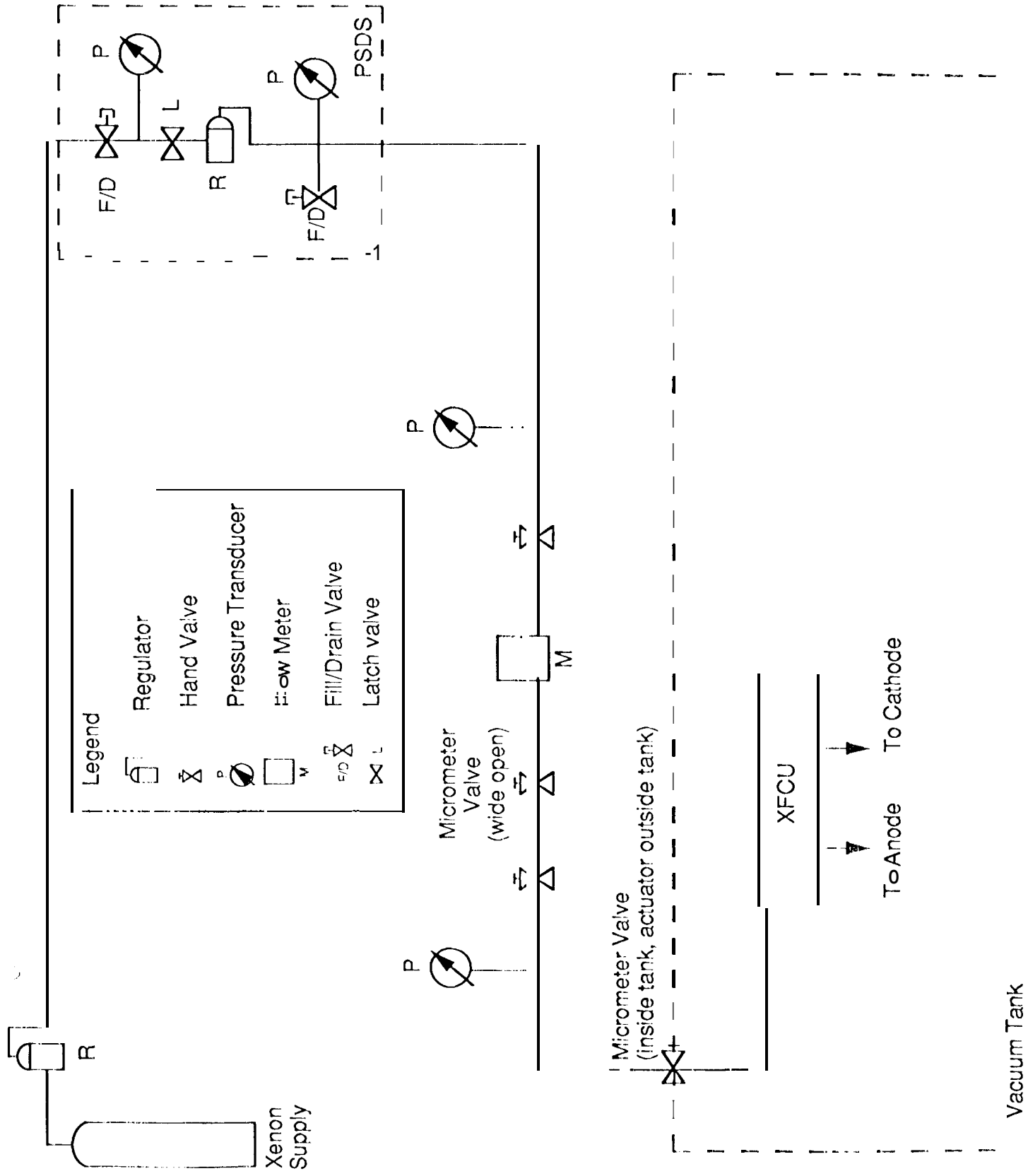


Fig 36

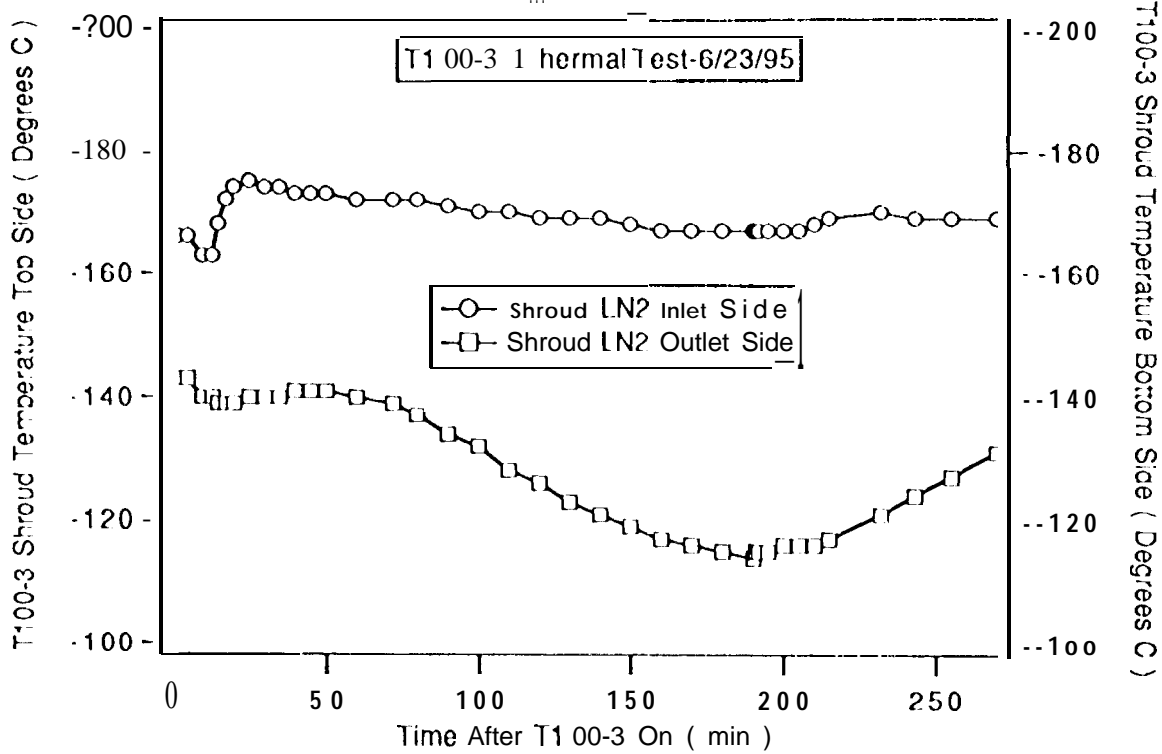
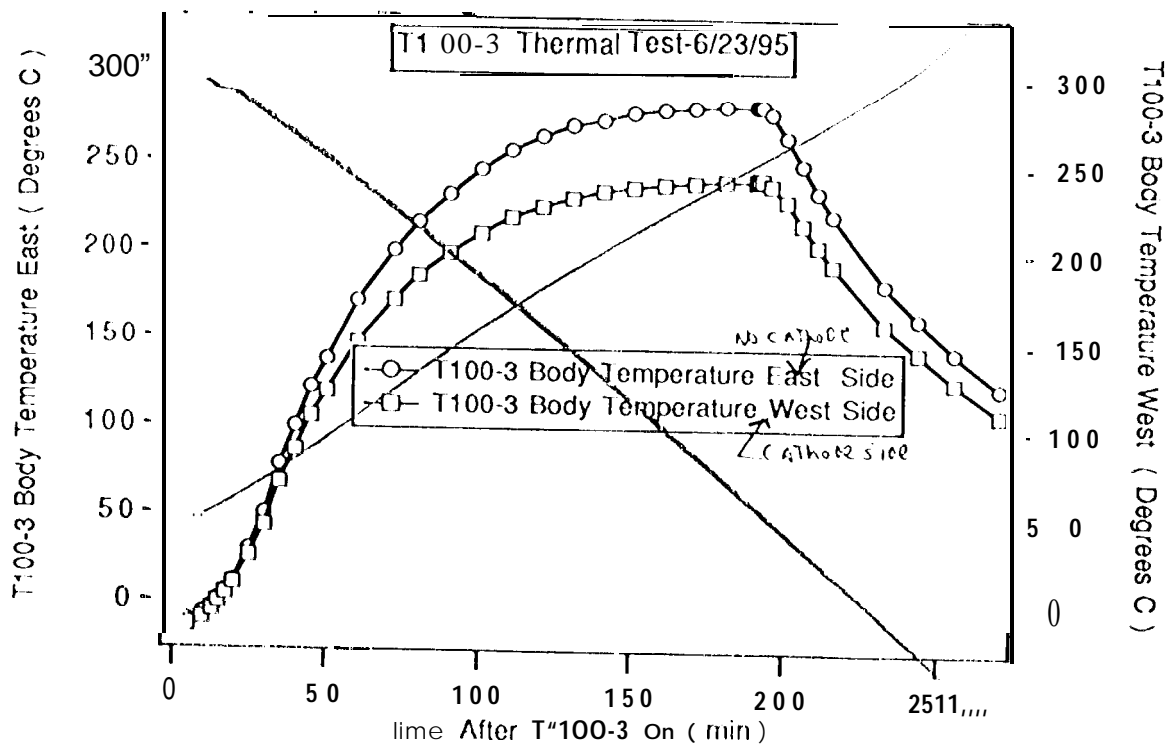
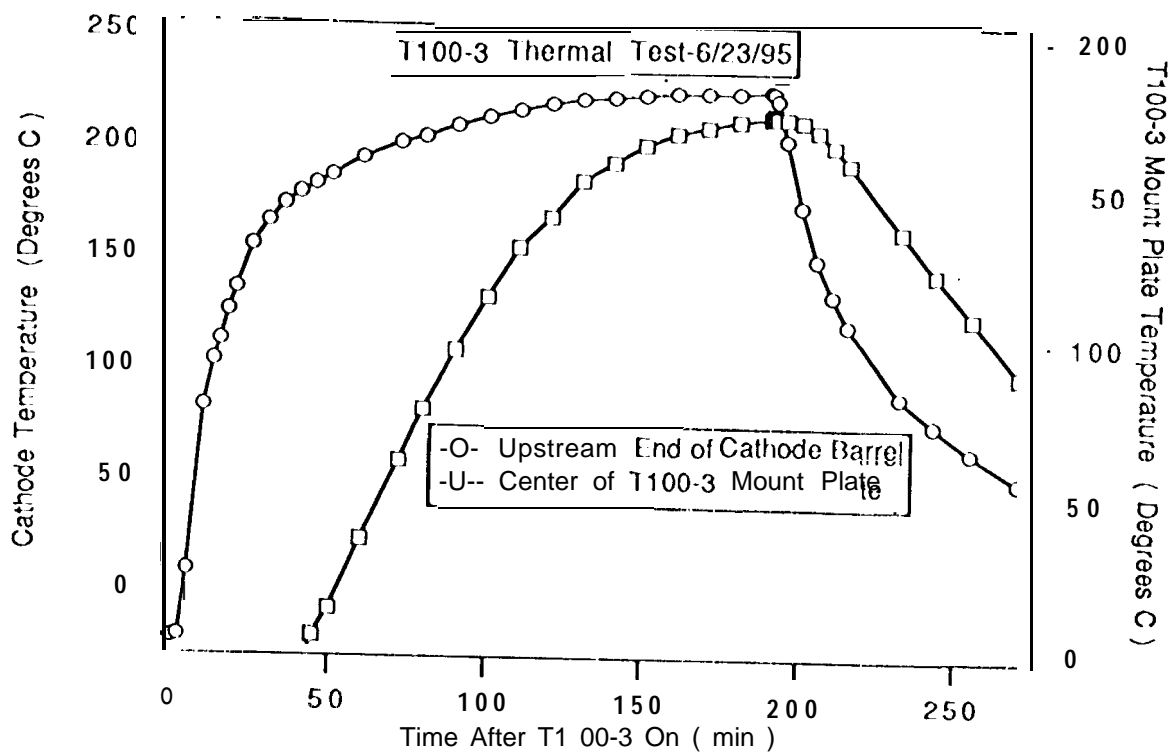


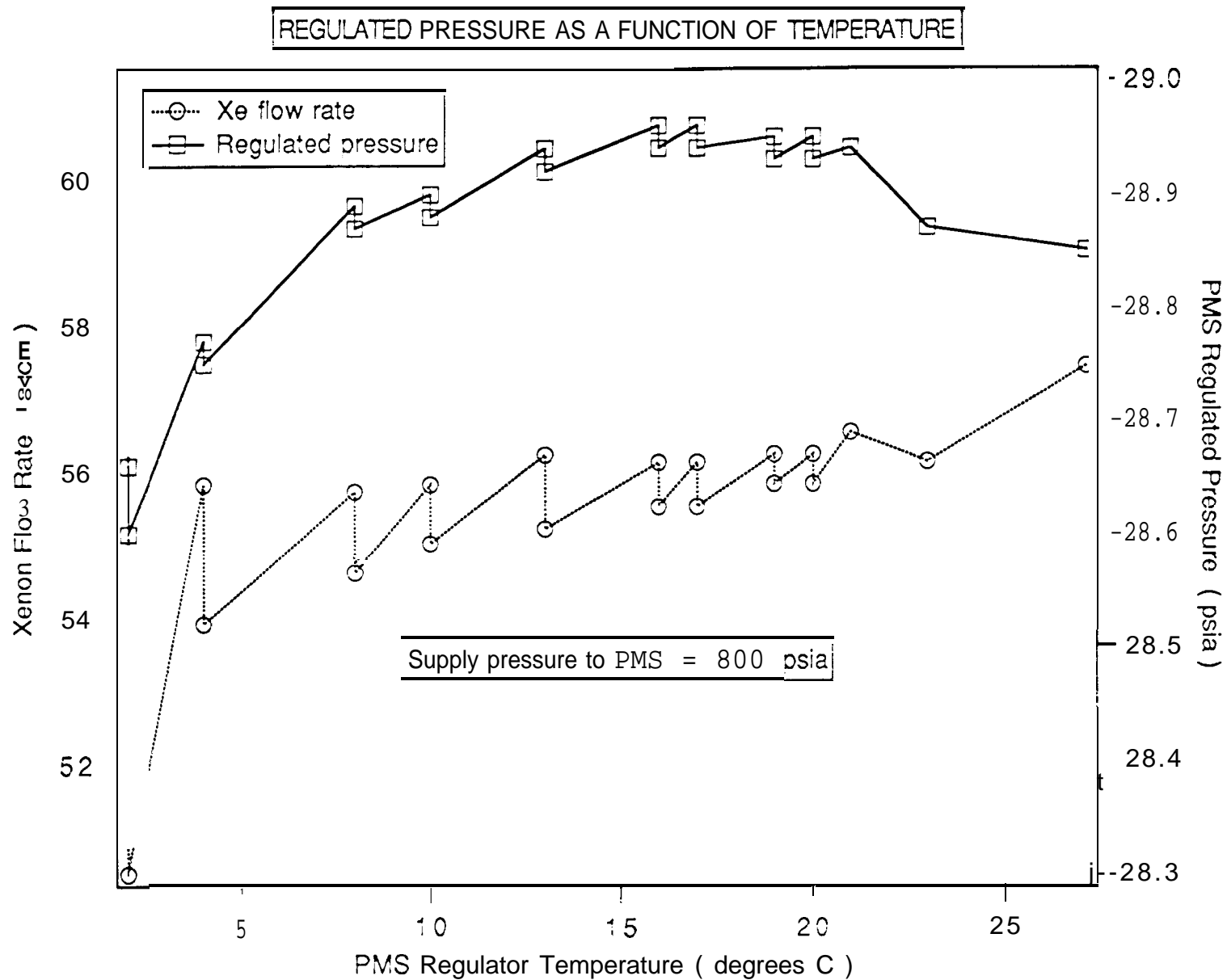
Fig 36

Fig 89 37



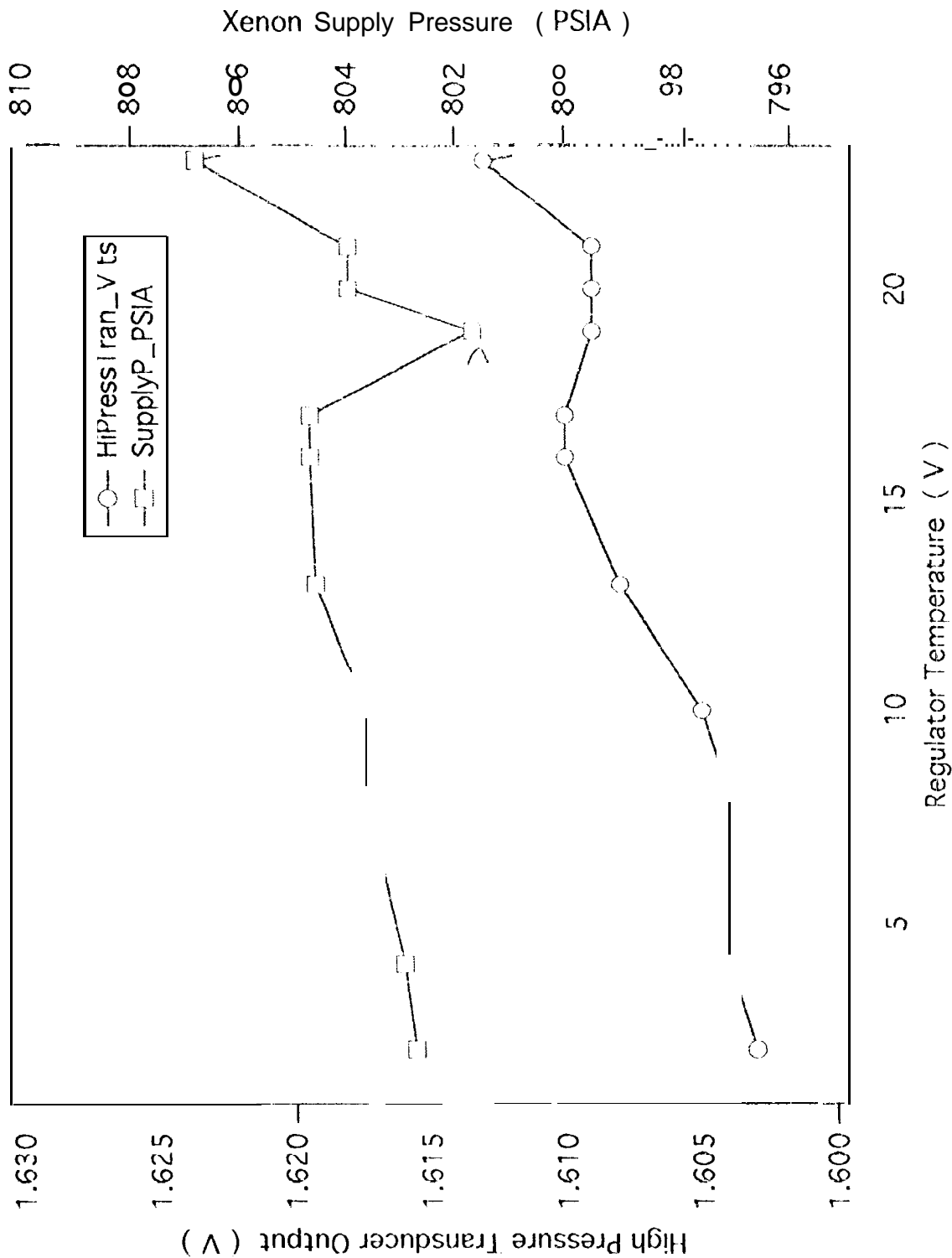


20. PMS Regulator



~~FIG 38~~ FIG 38

617 vms Table 2



~ KIS 401 39